The effect of halide and metal ions on the corrosion of aluminium in ethylene glycol solutions

Thesis

THE EFFECT OF HALIDE AND METAL IONS ON THE CORROSION OF ALUMINIUM IN ETHYLENE GLYCOL SOLUTIONS

By

ROBERT MARSHALL PRIGMORE

PhD THESIS

THE OPEN UNIVERSITY - FACULTY OF TECHNOLOGY

SEPTEMBER 1984

Date of Submission: Sept 84
Date of Award: 6.3.85

I hereby certify that the work described in this thesis has been carried out by the candidate under my general direction and supervision.

Dr. D.E. Davies,
Senior Lecturer -
Dept. Of Metallurgy
Swansea University.

Dr. M. Dorgham,
Senior Lecturer -
Dept. Of Technology
The Open University.

I hereby certify that this work has not already been accepted nor is it concurrently being submitted for any degree.

The work contained in Chapters 3 and 4 has been published.

R.M. Prigmore.

PERMISSION TO COPY

I declare that permission is given for the contents of this dissertation to be photocopied at the discretion of the library in which it is deposited.

R.M. Prigmore

ACKNOWLEDGEMENTS

I wish to thank Mr. M.J. Reilly, Mr. B. Phillips and Mr. J. Hart of Llanelli Radiators for their interest and sponsorship without which this research project would not have been possible.

Dr. D.E. Davies of Swansea University, my external supervisor, for maintaining an unfailing interest and giving me all the encouragement I needed to complete this work.

I would also like to thank Dr. M. Dorgham for his guidance on the administrative side of my project.

Last but not least I would like to thank Beth Rees for typing this thesis so accurately, and for understanding the work load involved.

SYNOPSIS

Aluminium components attached to an engine cooling system, will be exposed to 50% ethanediol coolant contaminated with metal cations and halide anions.

Since copper cations enhance the corrosion rate of aluminium, the effect of other metal cations of metals commonly found in the cooling system on the corrosion rate were evaluated. Aluminium samples were exposed to 50% ethanediol solutions containing various metals and metal cations.

Previous work has shown that halide anion size and concentration have an effect on the corrosion potential of aluminium, but the effects of metal cations have not been evaluated. A new corrosion cell was designed and built to evaluate these effects.

The nobility of the pitting potential of aluminium has been observed to decrease with chloride anion concentration and temperature increase in double distilled water. Potentiodynamic and potentiostatic experiments were therefore carried out to determine whether similar effects are observed with fluoride, bromide and iodide. Theoretically, if the penetration theory of pitting initiation is correct, then the nobility of Ep should increase with halide anion size.

It was concluded from the experimental work that:-

(1) Lead cations in the presence of chloride anions initiate corrosion of aluminium.

(2) Lead and copper cations in halide solutions shift the corrosion potential of aluminium to more noble values before deposition. Nobility continued to increase with metal cation concentration until the pitting potential was achieved and then levelled off. It is proposed that this effect is due to metal cations disrupting the outer Helmholtz plane.

(3) Ep values of aluminium in double distilled water and 50% ethanediol decreased in nobility with increase in halide concentration and solution temperature for all four halides.

(4) The fluoride Ep values were out of sequence, these values being as noble as those of iodide. A film was observed to form on aluminium exposed to the fluoride solution. It is proposed that this film increases the nobility of the pitting potential.

TABLE OF CONTENTS

TABLE OF FIGURES

LIST OF TABLES

CHAPTER 1

1.0 Development Of The Cooling System In Automobiles

1.1 Introduction

The first internal combustion engine was developed in the 16th Century and the fuel used to derive mechanical power was gun powder, these early experiments were not surprisingly abandoned. The early 18th Century saw experiments by the Frenchman, Etienne Lenoir, into gas driven engines. These gas engines conclusively demonstrated that the internal combustion engine was a practical and safe possibility.

The next step towards a practical automobile engine was taken by an Austrian, Siegfried Magnus, in 1873, the fuel of which was a mixture of benzene and air, exploded in a cylinder by an electrical spark.

Various experiments improved on this idea, until in 1878 Nicholas Otto, a German, worked out the system of the four stroke cylinder engine. The principle of the Otto engine is basically that most used today for internal combustion engines burning petrol. To withstand these explosive pressures, cast iron was selected for the cylinder blocks. The internal combustion engine system is illustrated in Figure 1.

The internal combustion engine as its name implies produces heat as well as mechanical energy; if the engine is to operate over long periods this heat has to be dissipated to the surrounding environment. Therefore, a system of internal pipe work was bored out of the cylinder head and engine block to carry coolant fluid through the engine. The heat energy absorbed was then transported via rubber pipes to a heat exchanger. A typical heat exchanger is illustrated in Figures 2 and 3.

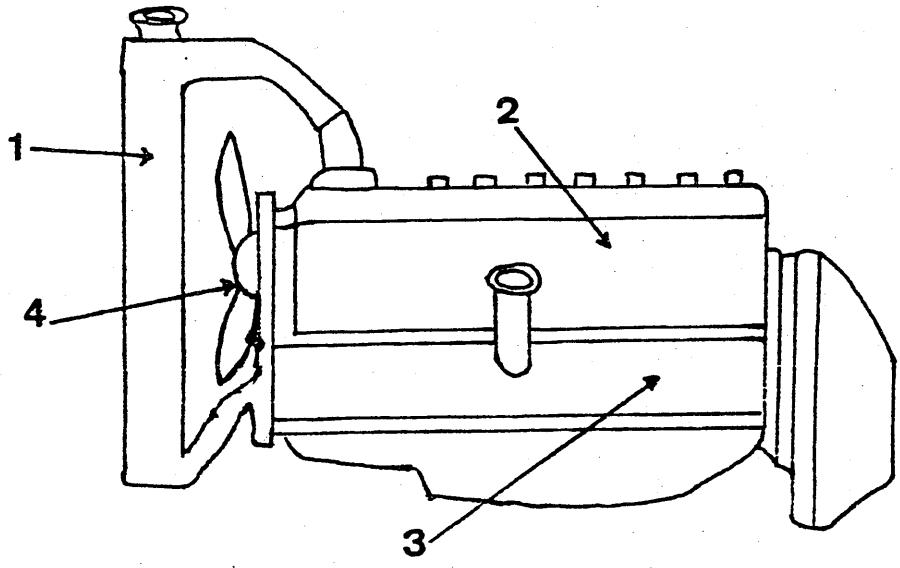

1 - Copper/brass heat exchanger.
2 - Engine head (cast iron).
3 - Engine block (cast iron).
4 - Cooling fan.

Figure 1 Internal Combustion Engine System

The heat exchanger is constructed from material of high heat conductivity, mainly copper and its alloys.

As can be seen from Figure 2, it consists of two end brass tanks connected by brass tubes to which gills, or airways, of copper foil are attached in horizontal rows. The whole structure is held together by solder joints.

The incoming hot coolant (approximately 85°C) is passed from one tank to the other, releasing heat energy by conductance through the brass tubes to the copper foil airways of high surface area. Air is blown continuously through these airways, hence dissipating the coolant heat energy to the environment. The coolant now of reduced temperature is passed back

FIGURE 2 Exploded view of Radiator core to illustrate the positions of the Copper Airways and Brass Tubes.

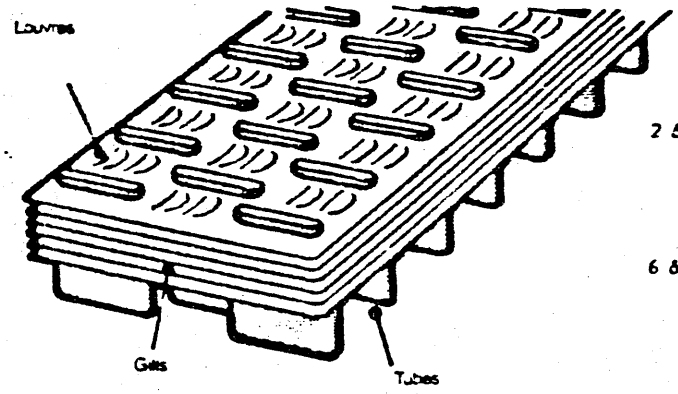

1) Heat exchanger core (Copper Airways, Brass Tubes)

2 & 3) Top and Bottom tanks (Brass)

4) Brass Oil Cooler

5) Brass Nut

6 & 7) Steel side support casing

8) Filler Cap

FIGURE 3

Diagram of a typical Heat exchanger

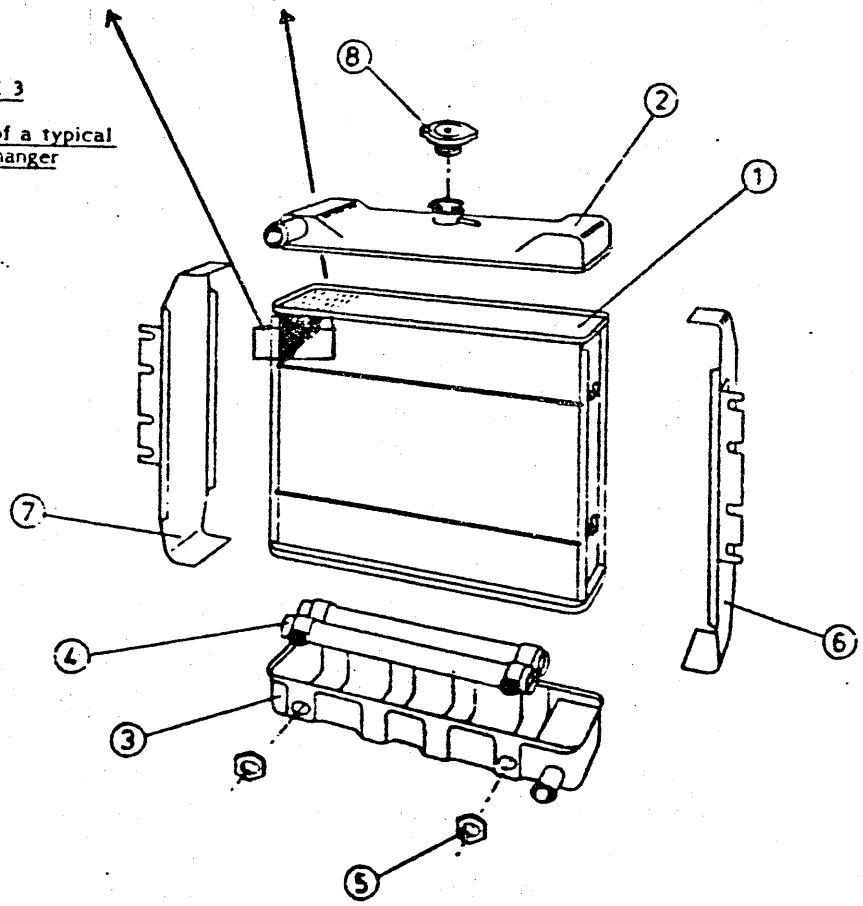

into the engine via the coolant pump to repeat this cycle.

Water was selected as the coolant and as temperatures on winter nights in the Northern hemisphere often drop well below the freezing point of water, engine damage occurred due to the expansion of ice which had formed in the cooling system.

Methods had to be found to overcome this major problem. Between 1922 and 1930 calcium chloride was added to the water as a freezing point depressant, but its use resulted in rapid corrosion of the engine and heat exchanger. In the early 1930's patents were granted for lard oil and glycerol as coolants of low freezing point suitable for use in an automobile cooling system. It was not until 1934 that Ethylene Glycol, now known as Ethanediol, was patented as a water soluble freezing point depressant, even though it had been reported by Curme and Young [21] in 1925 as a suitable freezing point depressant for the coolant used in internal combustion engines.

Due to the rapid rise in oil, and hence petrol prices, after the Suez Crisis, high priority was placed on fuel saving. With this aim in mind, alternative light-weight metals and alloys were investigated for use in the automobile engine system. Cast aluminium was found to be a successful replacement for the cast iron used for the engine head, and aluminium alloys such as AA 1070 were used along with glass reinforced plastics for heat exchangers.

Corrosion of the engine and heat exchangers by the coolant and its additives and contaminants which has always been a problem, was highlighted by the introduction of aluminium, a metal of low nobility,

into the cooling system.

The degree of corrosivity of the coolant, whether it is water or 50% ethanediol water mixture is enhanced by the presence of contaminants, both anions and cations.

1.1.1 Various Routes Of Contamination Of The Coolant

These are listed below along with their potential contaminants.

(a) Contaminated Make-Up Water

Chloride, sulphate and carbonate anions and magnesium and calcium cations can be introduced into the coolant from the tap water used for ethanediol dilution.

(b) Fluxing Operation

Two main types of fluxes are used for the joining together of the copper/brass components by lead/tin alloy solders during the assembly of heat exchangers.

(i) Zinc ammonium chloride water based solution.
This type of flux has been in use since the late 1930's. It leaves residues which are high in chloride salts.

(ii) Amine hydrobromide water based fluxes.
These fluxes have been in use since the early 1960's. They leave much less residue than the chloride based fluxes, these residues contain bromide salts.

Either one or both of these fluxes can be used to produce a completed heat exchanger.

Aluminium heat exchangers are normally constructed by using compression or crimp joints, but during the last five years brazing has become popular as a joining technique. Although brazing is understood to be the joining together of two metals as the result of melting a copper/zinc alloy it is not used in this context in this dissertation. Brazing in the case of aluminium heat exchangers is the joining together of two aluminium sheets by the melting and solidification of a thin film of aluminium silicon alloy on the surface of the sheets. This method was developed by Alcan at their research laboratories in Kingston, Ontario, Cooke and Bowman [35]. Some aluminium brazing fluxes contain fluorides and it is possible that under certain furnace conditions, residues containing fluoride salts can be left in the heat exchanger.

Both aluminium and copper/brass heat exchangers are sometimes found together in the same cooling system e.g. a copper/brass radiator and an aluminium heater or vice versa. It is possible, therefore, for an aluminium heat exchanger to be exposed to a coolant which is contaminated with the halides, fluoride, chloride or bromide either singly or in combination.

(c) Corrosion Of Metal In The Cooling System

Corrosion of the metals in contact with the coolant will contaminate the coolant with the respective metals cations. The potential cation contaminants are Pb^{2+} (lead), Cu^{2+} (copper), Zn^{2+} (zinc), Al^{3+} (aluminium), Fe^{2+} (iron) and Sn^{2+} (tin).

1.2 Localized Corrosion Of Metals

If metals which are potentially active, due to their reaction thermodynamics, such as aluminium and its alloys, are to be successfully exploited commercially, an air formed passive film which will resist environmental attack must be established and maintained on the surface. When a passive film has been fully established, the competitive reactions of film formation and film breakdown still proceed but their rates are in equilibrium, hence the film and metal are stable, due to the film's reaction kinetics.

However, if the passive metal sample is exposed to an electrolyte containing aggressive ions, and if the aggressive ion concentration and metal sample electrode potential both reach critical values simultaneously, the equilibrium reaction equation (1) will shift to favour the right hand side and the passive layer will break down and corrosion of the metal will take place.

$$M \rightarrow M^{x+} + xe^{-} \qquad (1)$$

It could be argued that passive film breakdown could be due to the aggressive ion decreasing the rate, or totally inhibiting the film repair reaction.

The critical potential or critical pitting potential is the most negative or least noble potential at which passivity just breaks down allowing corrosion to take place.

Various authors [1-3] have noticed a period of current oscillation before pit development, and it has been proposed that the electrochemical noise is related to the breakdown and repair events, with the breakdown reaction due to the aggressive ions eventually dominating the repair reaction. Therefore, it is related either to the rupture of the passive layer and its repair or to the formation of aggressive ion metal complexes on the metal surface leading to film breakdown by hydration of the complex salt.

The localized corrosion or pitting mechanism is made up of various processes occuring in sequence:-

(i) Initiation process leading to the breakdown of the passive layer.

(ii) Early stage of pit growth, involving negligible ohmic drop.

(iii) Later stages of pit growth, exhibiting appreciable voltage drops within the electrolyte in deep narrow pits and precipitation of a salt layer or hydroxide, from the saturated electrolyte in the pits, converting the pit into an occluded cell; i.e. a large pit with a very small restrictive opening.

However, the relative importance of these stages is still open to debate.

1.2.1 Initiation Of Localized Corrosion

Four main theories have been put forward to explain why a homogeneous solution on a flat metal surface of uniform composition could develop or initiate localized sites which have corrosion rates many orders of magnitude greater than the bulk of the surface. These are listed below and then individually reviewed.

(a) Penetration Mechanism.

(b) Adsorption Mechanism.

(c) Chemico-Mechanical Mechanism.

(d) Imperfection Theory.

1.2.2 (a) Penetration Mechanism

This mechanism was originally proposed by Evans [4] in 1927. The specific pitting tendency of the chloride ion he suggested was due to its small diameter which allowed it to penetrate the metal oxide film. This theory was based on experimental work by Britton and Evans [5] in which a potential was applied between two aluminium sheets placed in various metal salt solutions and the resultant current measured. The magnitude of the current flow for the various salt additions of equal molarities decreased in the order: $KCl > KBr > KF > K_2SO_4 > Na_3PO_4$. The authors concluded that the current flowing was a direct measure of the ability of the various anions to penetrate the aluminium oxide passive film layer. These results were probably complicated by some of the current flow observed being due to the dissolution of the metal sheets.

Considerable doubt was cast on this theory by Burwell and May [6]. In their work, they found that the penetration rate of chloride and the much larger nitrate ion through an isolated alumina film was almost identical. From this work, it was concluded that the aggressive nature of chloride anions towards aluminium is not only due to its small size and special penetrating ability.

A modified penetration theory by anion exchange with bound oxygen in the passive film lattice was suggested by Rosenfeld and Danilov [7]. The oxygen exchange takes place at sites where the oxygen bonding is at its weakest. After aggressive anions have displaced oxygen at the film surface they penetrate the passive film and concentrate at the metal/passive film interface initiating pitting.

Both the Evans and Rosenfeld penetration theories do not explain why passivity breakdown is localized. Hoar et al [8] put forward the suggestion that initially adsorption of the aggressive ions would occur at defective regions in the passive film such as grain boundaries and impurity zones in the metal. These adsorbed aggressive anions then enter and penetrate the passive film with the assistance of an electrostatic field across the film the strength of which is related to the pitting potential. Electrostatic field strength of 10^6v/cm should be possible in principle. Hoar and co-workers also believed that the ability of aggressive ions to penetrate the passive oxide film was related to their ionic radii, smaller anions having the highest rate of passage through the films. Therefore, fluoride anions should be more aggressive than chloride, bromide or iodide. These aggressive anion rich areas would then become areas of superior ion conductance, compared with the rest of the passive

film allowing rapid out-flow of metal cations at these sites, leading to localized corrosion.

Evidence for anion incorporation in passive films has been found by using surface analysis methods such as X-ray photoelectron spectroscopy (X.P.S.) or Auger electron spectroscopy (A.E.S.) in the case of aluminium, and secondary ion mass spectroscopy (S.I.M.S.) in the case of iron.

Chloride ions have been detected in the aluminium's passive film after exposure to chloride solutions [9,10] using (A.E.S.) and in iron surface film using (S.I.M.S.) [11], but it is true to say that other authors have failed to detect aggressive ions in exposed passive films of aluminium using (S.I.M.S.) [12] and iron by (A.E.S.) [13, 14] and iron and nickel using (X.P.S.) [15, 16]. This could be due to the metal surface treatment or cleaning process before analysis.

The passive film which forms on iron and nickel has been analysed at different depths by (X.P.S.) [15, 16]. The passive film was found to be made up of an outer hydroxide layer and an inner oxide layer. The oxide layer seemed to increase with the potential whereas the hydroxide layer thickness remained constant.

The non-barrier type hydroxide layer could very well be the exchange site for Rosenfeld and Danilov initiation theory, but penetration through the inner oxide layer would be required for pit initiation.

1.2.3 (b) Adsorption Mechanism

This mechanism has been put forward by Uhlig [17, 36], Kolotyrkin [18, 37], Hoar and Jacob [19]. These authors postulate that localized breakdown of passivity is due to the adsorption of aggressive ions such as halide anions locally on the passive film surface, causing an increased rate of hydration of the metal ions at these points, probably by complex salt formation with resultant thinning of the film in these areas. This reaction is obviously in competition with the normal repassivating oxidation reaction, hence the chloride concentration must have a critical minimum concentration level below which the oxygen adsorption reaction will dominate.

Recent work carried out by Khalil [20] demonstrated that the passive film on metals is thinned in the presence of chloride. Janik Czachor [14] also noticed thinning of the oxide film on iron samples after exposure to chloride by a coulometric evaluation of the remaining passive layer after galvanostatic reduction.

Work by Bohni and Uhlig [17] on the relationship of pitting potential to the thickness of the passive oxide film thickness revealed that the pitting potential was independent of film thickness. These results would seem to contradict the penetration theory because if this theory is correct, the thicker the oxide film the more noble the pitting potential, so this result, along with the oxide film thinning, seems to be in better accord with the adsorption theory rather than the penetration theory.

1.2.4 (c) Chemico-Mechanical Theory

This theory proposed by Sato [22], Hoar [23] suggests that the passive film is mechanically disrupted by the forces set up between adsorbed anions of like charge. These electrostriction forces then allow cracks to form in the passive film exposing bare metal, thus facilitating direct attack of the unprotected metal by the aggressive ion in the surrounding electrolyte, resulting in pit initiation.

There is little supportive evidence for this theory due mainly to the difficulty of differentiating between ion migration, penetration and chemico-mechanical ion action. No explanation of why these effects cause localized corrosion is given.

MacDonald et al [24, 38] proposed a separate chemico-mechanical theory based on the formation of voids at the metal/oxide interface, below sites of aggressive anion adsorption which allow high rates of outward metal ion flow. Accumulation of these vacancies form critical voids leading to rupture of the passive layer at these points.

1.2.5 (d) Imperfection Theory Or Flaw-Pit Theory

Wood et al [25, 39, 40] Zahavi and Metzger [41] propose that pitting corrosion is initiated at the base of imperfections in the passive film such as crevices, cracks, micro fissures and sub-surface cavities, where it is suggested that bare metal would be exposed for very short periods of time to the aggressive anions in the electrolyte.

In contradiction to this theory, Pearson et al [26], from an electron microscope study of pit formation in aluminium, found that irregularities

in the surface oxide film were not essential for pit formation and other factors must be taken into consideration. Imperfections are just sites of increased pitting susceptibility.

Again this theory does not offer any explanation as to the varying aggressive behaviour of the halide series of anions.

1.3 Early Stage Of Pit Growth Involving Negligible Ohmic Drop

After initiation, the corroding metal sample is covered by small pits 1 - 2 μm in diameter. There seems to be much debate on how growth between pit nucleation and fully active pits 1 mm in diameter and above, proceeds. It seems unlikely that the pH of the solution inside the developing pit could have dropped sufficiently to maintain the corrosion process, and due to the small size of the pit, ohmic drop between the pit base and sample surface of such small pits also seems unlikely to be able to sustain pit growth.

A review of localized corrosion by Gainer and Wallwork [27] suggests that a possible solution to this problem could be to look at pits below the minimum size and geometry required for sustained growth by either diffusion effects or ohmic drop as still part of the initiation process.

1.4 Later Stage Growth Of Pits (Pit Propagation)

Compared to pit initiation, pit propagation seems to be better understood; the auto-catalytic acid theory seems to be the most widely accepted theory of pit propagation. This theory is based on the fact that the hydrolysis reaction of cations having sparingly soluble hydroxides, will lead to the generation of local acidity.

$$Al^{3+} + 3H_2O \rightarrow Al(OH)_3 + 3H^+ \qquad (2)$$

Hoar [42], Pourbaix [28] identified the importance of this reaction in pitting. The insoluble metal hydroxides or metal salts formed deposits over and around the developing pit, decreasing the pit orifice diameter, and restricting free diffusion of the electrolyte between the forming

pit and the surrounding bulk electrolyte.

This restricted interchange of electrolyte accelerates the pH decrease inside the pit, allowing the pH to drop below a point where direct chemical attack of the pit wall will occur. This process becomes auto-catalytic because the acid concentration in the growing pit becomes strong enough to attack the metal directly, reaction 3.

$$M^{x} + xH^{+} \longrightarrow M^{x+} + \tfrac{1}{2}xH_2 \qquad (3)$$

The metal cations formed during the acid dissolution reaction will be hydrolysed, to form more acid H^{+} ions thus perpetuating the corrosion reaction cycle, reaction 4.

$$M^{x+} + xH_2O \longrightarrow M(OH)_x + xH^{+} \qquad (4)$$

This auto-catalytic effect allows pitting corrosion to continue even when the potential is moved into the passive region. Suzuki et al [29] showed that the pH of artificially formed pits on stainless steel samples exposed to 0.5 N sodium chloride solution were in the range pH 0.6 - 0.8, and Szklorska and Smialowska [30] determined pH values as low as 1.3 in naturally formed pits on stainless steel exposed to chloride containing solution, the bulk solution pH being 6.5. The pit electrolyte pH values determined by both authors are well within the range required for direct acid attack on the base metal, and hence initiate the auto-catalytic reaction cycle. Ohmic drop between the pit base and metal surface of large well developed pits has also been put forward as a driving force for pit propagation. Pickering and Frankenthal [31] suggest

that this ohmic drop could be caused by the presence of a hydrogen bubble within the pit, which gives rise to a high resistance path at the constriction that exists between the bubble and the bottom of the pit, resulting in a large I.R. drop.

1.5 Localized Corrosion Of Aluminium

From a thermodynamic stand point, aluminium is a highly reactive metal which should spontaneously oxidise to form alumina Al_2O_3, but in reality high purity aluminium has good corrosion resistance properties. Alloying aluminium or increasing concentration of impurities usually reduces the corrosion resistance, as most metal additions are usually cathodic to aluminium possibly setting up surface galvanic cells.

The good corrosion resistance already mentioned is due to a protective skin of aluminium oxide, which forms on exposure to an environment containing free oxygen. This alumina film then restricts further movement of unreacted oxygen to the metal's surface, slowing down the oxidation reaction not totally inhibiting it. Therefore, aluminium is stable due to its reaction kinetics.

Alumina Al_2O_3 is amphoteric and will dissolve in alkaline or acid solutions. Work carried out by Pryor [32] on the corrosion potential of aluminium exposed to mixtures of hydrochloric acid and sodium hydroxide solutions, saturated with oxygen, demonstrated that the corrosion potential of aluminium is largely pH independent up to pH10. At a higher pH than 10, the aluminium's potential moves in the active direction, with the following reaction (5) taking place. Figure 4.

$$Al + 2OH^- \longrightarrow AlO_2 + 2H^+ + 3e^- \qquad (5)$$

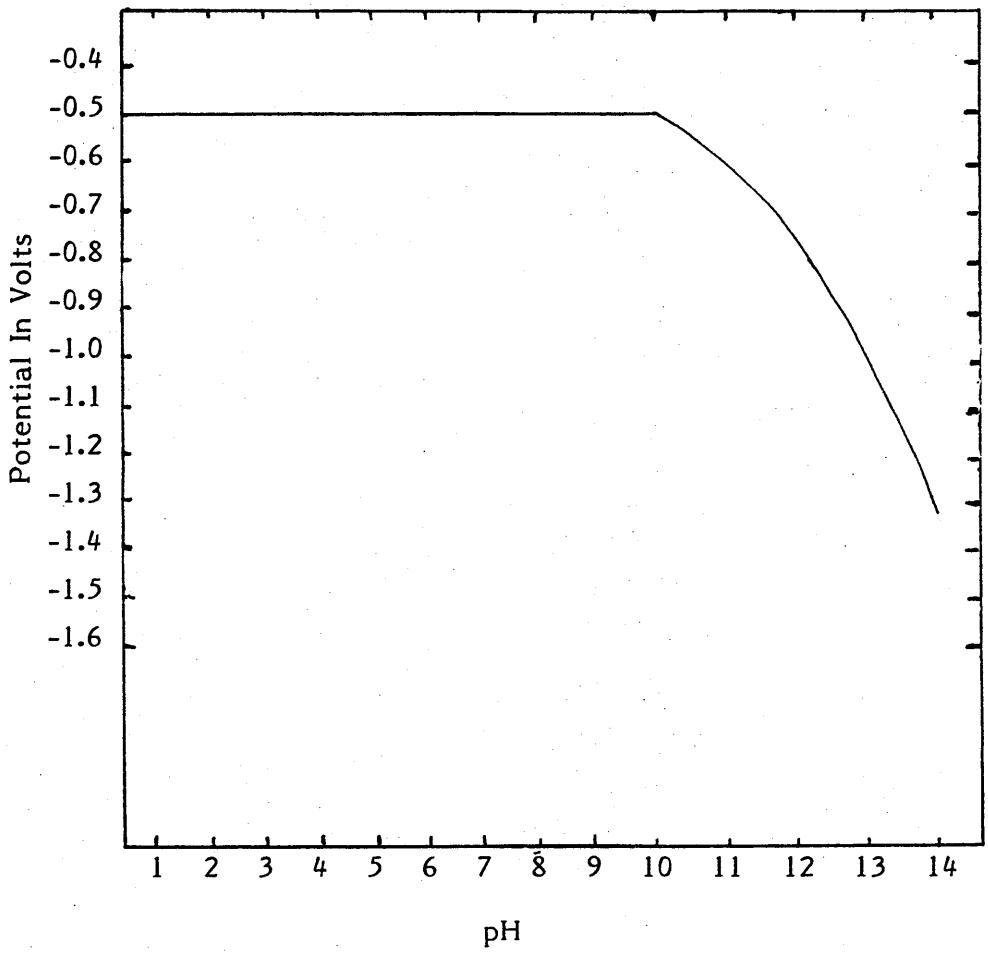

Figure 4 Relationship Between Potential And pH For Aluminium

These corrosion potential results imply that except at pH values in excess of pH10, the corrosion reaction kinetics of aluminium are always strongly influenced by the thin film of alumina Al_2O_3.

The passive aluminium oxide film which forms on aluminium exposed to the atmosphere is between 20 - 100 Å thick and highly uniform. High energy electron diffraction studies carried out on the air-formed film by Pryor to determine its structure, proved that the film was

F.C.C. gamma Al_2O_3 which had low crystalline order and was almost amorphous.

This amorphous F.C.C. gamma Al_2O_3 has a surprisingly high level of ionic resistance compared with crystalline gamma Al_2O_3.

The stoichiometric gamma Al_2O_3 unit cell contains 32 oxygen ions in a F.C.C. lattice and there must also be an average of $21\ ^1/_3$ aluminium ions per unit cell disposed between 24 available lattice sites, 16 octahedral and 8 tetrahedral. Therefore, there must be $2\ ^2/_3$ uncharged vacancies in the cation lattice per unit cell; this is the reason why crystalline gamma Al_2O_3 has such a low ionic resistance. Pryor accounts for the high ionic resistance of amorphous air-formed Al_2O_3 films, by proposing that the excess aluminium ions in the vicinity of the interface are positioned on what otherwise would have been vacant sites in the cation lattice of stoichiometric gamma Al_2O_3. Electrical neutrality is, of course, maintained by the provision of three partly bound electrons for each excess aluminium ion so substituted. The structure of the thin air-formed film is that of gamma Al_2O_3 with excess aluminium ions in normally vacant cation sites.

This defective gamma Al_2O_3 has:-

(i) a high ionic resistance;

(ii) low electronic resistance with resistivity increasing with increasing distance from the metal oxide interface;

(iii) very poorly developed long range order.

Pryor then compared the impedance of the air–formed aluminium oxide film at various frequencies before and after exposure to aqueous chloride solutions. At a frequency of 1 kHz the impedance dropped substantially after exposure but the impedance at 100 kHz remained unchanged. Impedance/frequency profiling of anodised aluminium with a thick film 270 $\mathring{A}$, before and after exposure to aqueous chloride was then carried out. From the results of both experiments it was seen that after immersion in sodium chloride solution, the ionic resistivity had dropped but the electronic resistance had remained the same.

It was proposed that the foregoing electrical results can be explained in that electrical neutrality is restored by the passage of 1 aluminium ion from that lattice into solution for each 3 chloride ions entering the oxide lattice, in replacement for 3 oxygen ions, reaction (6).

$$Al^{+++}(L) + 3O^{--}(L) + 3Cl^{-}(S) + 6H^{+}(S) = Al^{+++}(S) + 3Cl^{-}(L) + 3H_2O \qquad (6)$$

where L = Lattice Position, S = Solution

This reaction is basically chloride entry into the passive film by oxygen exchange, this exchange reaction creating additional uncharged cation vacancies which permit enhanced rates of transport of aluminium ions through the continuous gamma Al_2O_3 film, hence initiating localized corrosion.

Verkerk[33] proved that chloride anions are taken up into the anodic gamma Al_2O_3 films formed in boric acid, by immersing the anodised aluminium

into tagged sodium chloride solution and scanning the exposed surface for radioactivity. Verkerk found that the radioactive chloride ions were distributed non-uniformly in the anodic oxide. He also found that the points of highest chloride ion concentration pitted earliest.

From the results of work by Pryor [32], Verkerk [33], and reviews of localized corrosion by Gainer and Wallwork [27] and H.H. Strehblow [34] it seems certain that aggressive ions interact with the passive gamma Al_2O_3 film either by adsorption onto the surface or by penetration of the film. There still seems to be very little evidence to ascertain why the aggressive anion actions are localized, but selected incorporation at areas of weakness such as dislocations and cracks, seems to be the most likely explanation.

Due to the low solubility of aluminium hydroxide and the ease of hydration of aluminium cations, the autocatalytic theory of pit propagation would seem to be an acceptable method of pit growth.

Aluminium hydroxide precipitate probably blocks the pit's orifice, forming an occluded cell very early on in its development. This prevents or restricts free exchange of pit electrolyte with the bulk electrolyte allowing rapid build-up of acidity inside the pit.

Pourbaix's theory [28] that the metal surface acts as an aerated cathode and the pit surface acts as a non-aerated anode is probably a good general explanation of why small pits formed at the initiation stage develop into large pits, which are able to maintain growth due to acidity levels within the pit.

1.6 Critical Pitting Potential

The critical pitting potential is usually defined as the most negative or least noble potential at which passivity first breaks down allowing localized corrosion to take palce.

The critical pitting potential is described variously as break through or breakdown potential, pitting potential [8, 43 - 47], critical pitting potential [36, 48, 49], critical potential for pit formation [37], activation potential [48,56] and protection potential [44]. It can be determined by different electrochemical methods, and usually the results obtained for similar metals or alloys in similar environments do not agree.

The critical pitting potential (Ep) is determined by measurements of the anodic polarization curve using a potentiostat. From an analysis of electrochemical methods by Smialowska and Czachor [51], there are three variations of this method:-

(i) The stationary method. In this technique a fresh sample of the metal under investigation is held at an assigned potential until a constant current is established. This current is then recorded and a graph of potential against current built up from a large number of such determinations over a wide potential range.

(ii) Potentiokinetic or Potentiodynamic. In this technique the potential is changed gradually by a motorised drive system, the current being recorded by a pen recorder.

(iii) Quasi-Stationary. In this technique the potential of the test sample is changed in equal steps of potential, the current being recorded continuously by a pen recorder.

The net result of all three methods is a trace of potential against current similar to Figure 5.

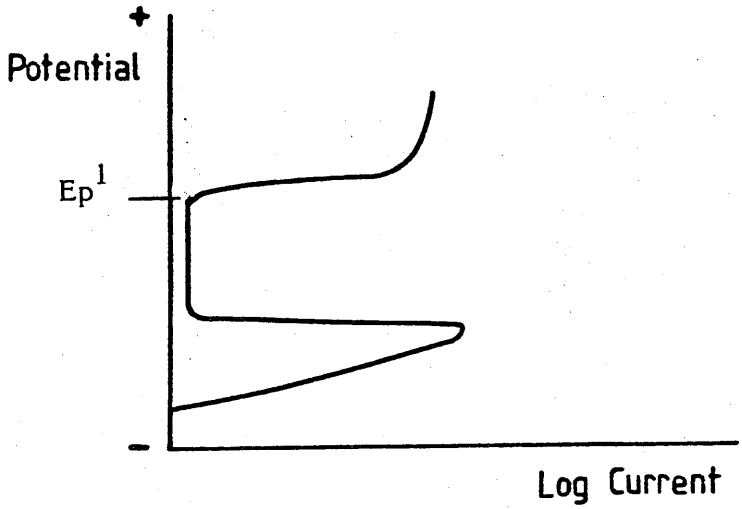

Figure 5

Schematic representation of the anodic polarization curve I vs E of a metal in solution containing aggressive ions obtained using a potentiostatic device.

Ep being the potential at which the current and hence the corrosion rate rises rapidly, indicating the initiation of pitting or the breakdown of passivity.

In their analysis, Smialowska and Czachor propose that there is not one but two pitting potentials. When the potential scan is reversed using the same freely corroding sample, the repassivation potential Ep^2 is not the same as the potential for passivity breakdown Ep^1, Figure 6.

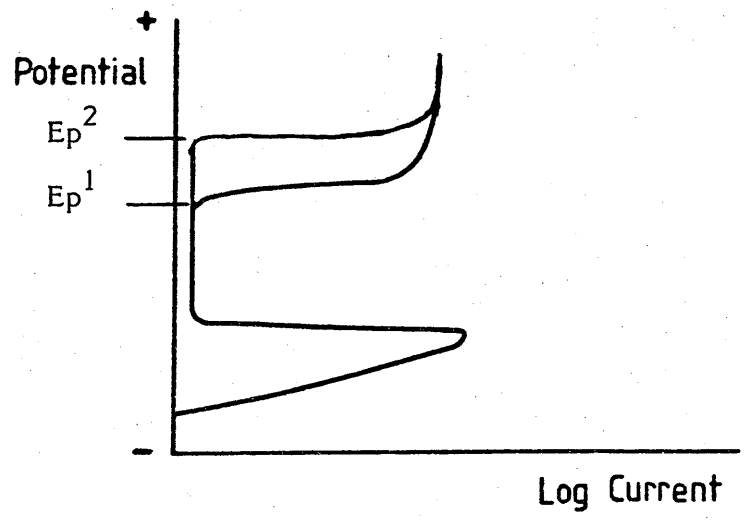

Figure 6

Schematic representation of the forward anodic polarization curve I vs E superimposed on the reverse anodic polarization curve of a metal in solution containing aggressive ions.

The authors termed Ep^1 the pitting nucleation potential and Ep^2 the critical pitting potential, but state that the tendency of a metal to pitting in a given medium can be characterized by both Enp and Ecp determinations. The electrochemical technique used in this dissertation to evaluate the pitting potential, determined the Enp or pitting

nucleation potential.

Leckie's [48] data shows that the Enp value determined depends on the rate of potential change. The cause of this phenomenon was discussed in detail by Schwenk [52]. He observed, as did other authors [53 - 56], that the more noble the potential, the shorter the induction time for pit formation.

From a review of pitting corrosion by Sutton [57], it is seen that the critical pitting potentials of aluminium have been determined by various workers the values obtained by Ergang and Masing [58, 59] are typical.

Table 1

Critical Potentials

Solution	Ep	Solution	Ep
0.01 N NaCl	- 470 mV	0.002 N NaBr	- 260 mV
0.1 N NaCl	- 600 mV	0.02 N NaBr	- 330 mV
1.0 N NaCl	- 700 mV	0.2 N NaBr	- 550 mV
0.5 N NaCl	- 500 mV	0.77 N NaBr	- 610 mV

(All potentials are relative to a saturated calomel electrode.)

These results show that the Ep value decreases in nobility with increase in aggressive anion concentration and with the increase in aggression of the anion i.e. chloride more aggressive than bromide.

Work by Kaesche [60] and Uhlig [36, 17] showed that the value of Ep varies linearly with Log Cl^- concentration.

1.7 Corrosion Potential

This is the natural potential (no applied current) Ecorr of a metal or alloy exposed to a conductive electrolyte.

Localized corrosion of metals exposed to various electrolytes will only occur if the corrosion potential of the metal is shifted to a value more noble than the critical pitting potential, either naturally or by an applied current. Therefore, any factors which cause a natural movement of the corrosion potential will be of importance in considering the stability and life expectancy of metals exposed to the environment.

Khairy and Hussinn [61] investigating the influence of anion concentration on Ecorr values of aluminium in sodium chloride solutions, found that the corrosion potential changed from ca - 590 mV in 10^{-3} N solution to - 840 mV in a saturated solution.

Pryor [62] also studied the effect of anion type and concentration on Ecorr. He used two sets of specimens; the first set was abraded in a closed apparatus having an atmosphere of helium to prevent re-oxidation of the surface, before immersion in the test solution; the second set was also abraded but then left for 2 hours in dry air to allow an oxide surface film to form. Upon immersion, the potentials of the film free specimens rose sharply from very low values, and after 15 minutes attained a steady value. The specimens which had oxide surface films showed much higher initial potentials, which rose only slightly to attain the same steady values as those of the film free specimen.

The constant values obtained after 100 minutes immersion are shown in Table 2.

Table 2

Corrosion Potentials After 100 Minutes [62]

Solution	Potential	Solution	Potential
0.1 N NaI	- 550 mV	1.0 NaI	- 650 mV
0.1 N NaBr	- 565 mV	1.0 NaBr	- 675 mV
0.1 N NaCl	- 720 mV	1.0 NaCl	- 790 mV

The results show that potential is primarily dependent on the presence of an oxide film but that there is also dependence on the anion type and concentration. The order of aggressiveness of the anions decreases in the order Cl^- : Br^- : I^- as shown by the trend in corrosion potentials.

Increasing the concentration of a given anion raises the aggressiveness of the solution and lowers the corrosion potential to more active values.

Haynie and Ketcham [63] carried out a similar investigation and found the same pattern of results.

CHAPTER 2

2.0 Corrosion Behaviour Of Metals And Alloys Used In The Construction Of An Automobile Cooling System In 50% Ethanediol And Drinking Water

2.1 Introduction

From the illustrations Figures 1, 2 and 3, of the automobile engine and heat exchanger layout, it can be seen that the metals aluminium, cast iron, brass, lead/tin solders and copper are all exposed to the circulating coolant whether it be water or 50% ethanediol water solution. Therefore, the soluble cations of one metal can interact with the surfaces of the other metals in contact with the coolant, thus leading to the enhanced corrosion rate or the initiation of corrosion on otherwise stable metal surfaces (notably aluminium).

Some of the metals and alloys are in electrical bimetallic contact e.g. cast aluminium to cast iron, brass to solders, copper to solders. These combinations lead to an increase in the corrosion rate of the least noble metal or alloy of the combination.

The following experiments are designed to evaluate the corrosion rate of metals used in the construction of automobile engine systems on their own and in bimetallic contact with other metals in 50% ethanediol tap water solutions. The experiments also study the initiation of corrosion and the enhancement of corrosion rate due to metal cation/ metal surface interaction.

The chemical analysis of the tap water used throughout this dissertation is given in Table 3.

Table 3

Tap Water Analysis

Determinand Name	Result
pH	7.3
Conductivity (20°C) (μS/cm)	176.0
Dissolved Solids (180°C) (ppm)	116.0
Total Hardness (ppm $CaCO_3$)	56.2
Total Alkalinity (ppm $CaCO_3$)	29.0
Chloride (ppm Cl)	22.0
Dissolved Silicate (ppm SiO_2)	1.8
Dissolved Sulphate (ppm SO_4)	16.0
Dissolved Sodium (ppm Na)	8.8
Dissolved Potassium (ppm K)	2.6
Total Copper (ppm Cu)	0.02
Dissolved Magnesium (ppm Mg)	3.12
Dissolved Calcium (ppm Ca)	17.4
Total Zinc (ppm Zn)	0.01
Total Aluminium (ppm Al)	0.05
Total Lead (ppm Pb)	0.02
Total Manganese (ppm Mn)	0.01
Total Iron (ppm Fe)	0.09

2.2 Metal Test Samples

The metals and alloys selected for use throughout all these experiments are identical to those commonly used in the construction of the automobile engine cooling system.

These metals are listed below along with their respective chemical analyses, and their uses in the construction of an automobile cooling system.

Aluminium (Used to manufacture heat exchangers)

Magnesium	0.005%
Copper	0.01%
Iron	0.28%
Manganese	0.02%
Silicon	0.12%
Titanium	0.01%
Chromium	0.01%
Aluminium	Rest

Lead (Raw materials for solder alloys)

99.99% Pure

Tin (Raw materials for solder alloys)

99.99% Pure

Brass (Used for manufacturing tube plates, tubes and tanks for heat exchangers)

Copper	69.80%
Zinc	30.10%
Lead	0.05%
Iron	0.05%

Cast Iron (Used to manufacture the engine block)

Carbon	3.10 - 3.45%
Silicon	1.85 - 2.45%
Manganese	0.6 - 0.90%
Sulphur	0.12% max.
Nickel	0.25%
Iron	Rest

Solders

	Tin %	Silver %	Antimony %	Lead %	Comments
LTS P (From Working Solder Pit)	1.4	0.48	0.12	Rest	Used for:-
LTS (Standard)	2.5	0.45	0.05	Rest	Tube to Tube
30% Tin Solder	30.0	-	-	Rest	Plate Joints.
15% Tin Solder	15.0	-	-	Rest	Tube to Copper Airway Joints.

Note: LTS is an abbreviation for Lead Tin Silver.

LTS P represents LTS Solder which has been used in a working solder pit for 1000+ working hours, and hence has a reduced tin content.

2.2.1 Test Sample Cleaning

The solder samples were cleaned by boiling in 10% acetic acid solution for one minute, then rinsed in cold water and dried to constant weight. This operation was performed before and after test solution exposure.

The brass, aluminium and cast iron samples were degreased in acetone and dried to constant weight before test solution exposure. After solution exposure, they were brushed lightly under running water to remove any surface deposits, and then dried to constant weight.

2.3 Laboratory Trial To Determine The Corrosion Rates Of Metal Components Commonly Found In An Automobile Cooling System In Uninhibited 50% Ethanediol

The metal samples were in the form of square sheets 2.5 cms side which had locating holes drilled in them. Their areas and weights were determined and recorded. The samples were then placed on a glass rod and were separated by plastic, non-conductive clips, to form a sample rig. The rig, Figure 7, was immersed in a beaker containing 450 mls. of 50% ethanediol solution.

The following metal samples from section 2.2 were used in this experiment.

Lead	99.99%
Aluminium	
30% Tin Solder	
Cast Iron	
Brass	
2.5% Tin Solder (LTS)	

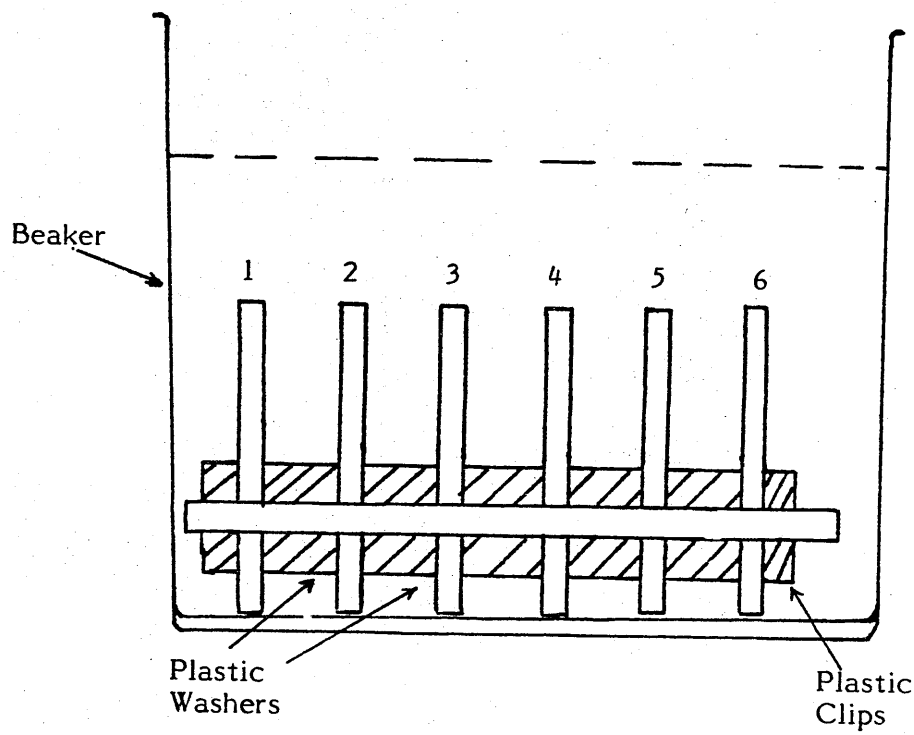

1 - Aluminium.
2 - Iron.
3 - Brass.
4 - Lead.
5 - 30% Tin Solder.
6 - 2.5% Tin Solder (L.T.S.).

Figure 7 Diagram Of Corrosion Rig Containing Metal Samples Commonly Found In The Automobile Cooling System

2.3.1 Trial Conditions

(a) The beaker containing the test rig was placed in an oven for ten days at 85° C. The oven was switched off each day for two hours to simulate engine stop periods and cold starts.

(b) The solution was made up using tap water of the composition given in Table 3.

(c) The solution was topped-up each day to maintain standard conditions.

2.3.2 Results

The results are given in Table 4.

Table 4

Solution	Metals	Weight Loss
50% Ethanediol	Lead	23.0 mg/cm^2
	Aluminium	0.5 mg/cm^2
	30% Solder	5.0 mg/cm^2
	LTS Solder	20.0 mg/cm^2
	Iron	4.0 mg/cm^2
	Brass	0.5 mg/cm^2

2.3.3 Conclusions

(a) The lead and lead-tin alloys together with iron suffered the highest rate of corrosion which was uniform in nature. The pure lead metal and the low tin solder suffered a much higher rate of attack than the higher tin solder (30% tin), indicating that increasing tin percentage in solder gives increased corrosion resistance.

(b) The weight loss of the brass was only 0.5 mg/cm^2 and no visible surface attack could be observed.

(c) Although the aluminium sample appeared to have a low rate of corrosion, the attack which did occur was localized in nature producing large numbers of pits and pinholes. The surface was also discoloured due to the deposition of a thin layer of lead.

(d) The various rates of attack indicate that the metal cations available in solution for surface interaction are:- Pb^{2+} (lead), Al^{3+} (aluminium) and Fe^{2+} (iron).

2.4 The effect of contact with brass on the corrosion rate of lead/tin solders of varying tin content.

The following metal samples in the form of sheets of 2.5 cms side which had locating holes drilled in them were tested in two corrosion rigs, Figures 8 and 9. All the metal samples had their weights recorded before and after the corrosion trial, in three hundred mls. of 50% ethanediol solution in tap water.

LTS Solder	30% Tin Solder
LTS P	Brass
15% Tin Solder	

One corrosion test rig was built by threading the solder samples onto a glass rod and separating them from each other by brass washers (Figure 8). The second test rig was similar but plastic insulating washers were used to separate the solder samples (Figure 9).

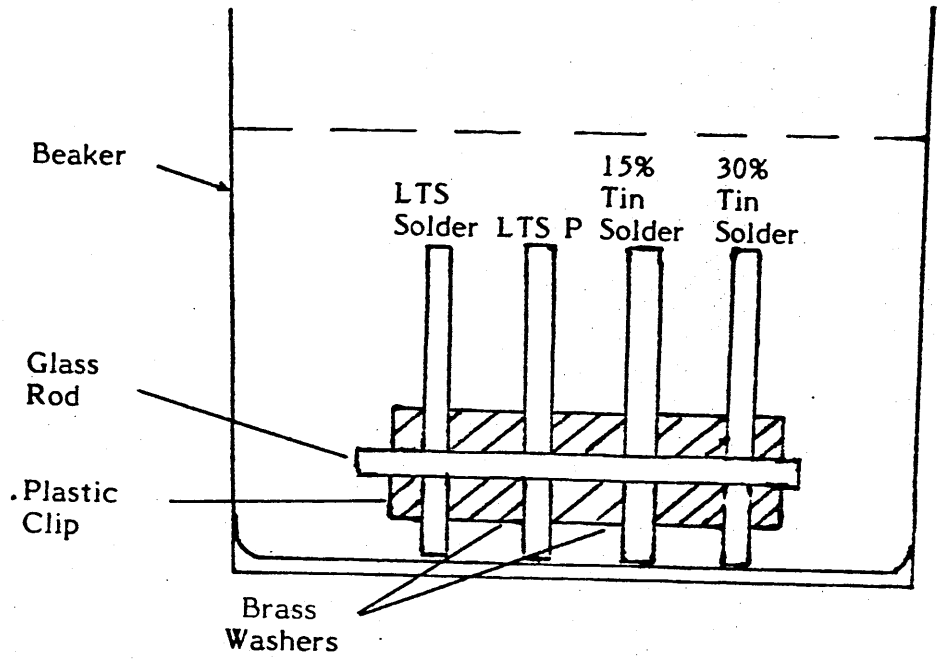

Figure 8 Diagram Of Corrosion Rig Containing Samples Of Automobile Solders Separated With Brass Washers.

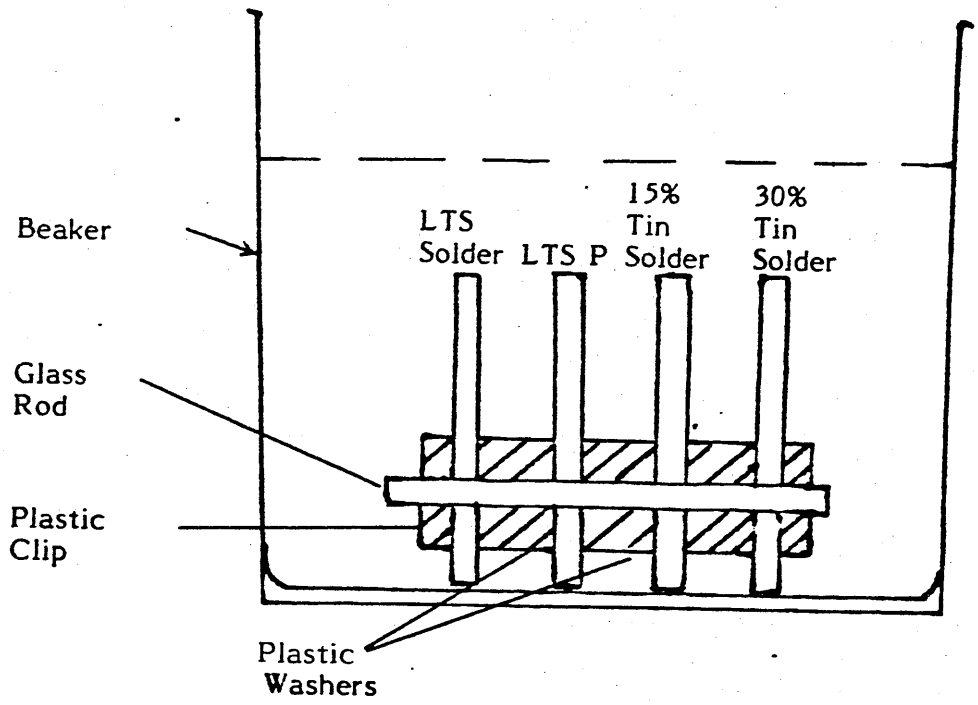

Figure 9 Diagram Of Corrosion Rig Containing Samples Of Automobile Solders Separated With Plastic Washers

2.4.1 Trial Conditions

(a) The two solder rigs were placed in the 50% ethanediol solutions and kept at 85°C for fourteen days.

(b) The oven was switched off every day for two hours to simulate engine stop periods and cold starts. The solution levels were also topped-up at this point with double distilled water.

(c) The concentration of the metal cations, lead, copper, zinc and tin were determined and recorded for each of the two rig solutions after the fourteen day trial period.

At the end of the trial period, the metal samples were removed, cleaned and their final weights were recorded and used to calculate the rate of corrosion over the fourteen day period for each metal.

2.4.2 Results

The weight loss of the various solders is given in Table 5.

Table 5

Test Rig Number	Metal or Alloy	Weight Loss Rate Over Fourteen Day Period
1 (Brass Spacers)	LTS P	3.38 mg $cm^{-2}d^{-1}$
	LTS	1.72 mg $cm^{-2}d^{-1}$
	15% Tin Solder	0.60 mg $cm^{-2}d^{-1}$
	30% Tin Solder	0.20 mg $cm^{-2}d^{-1}$

Test Rig Number	Metal or Alloy	Weight Loss Rate Over Fourteen Day Period
2	LTS P	1.53 mg $cm^{-2}d^{-1}$
(Plastic Spacers)	LTS	0.92 mg $cm^{-2}d^{-1}$
	15% Tin Solder	0.26 mg $cm^{-2}d^{-1}$
	30% Tin Solder	0.12 mg $cm^{-2}d^{-1}$

After the fourteen day trial period, the solutions were analysed and the results given in Table 6 below.

Table 6

Metals	Test Rig Number 1	Test Rig Number 2
Lead	181.00 ppm	40.00 ppm
Copper	0.17 ppm	0.4 ppm
Zinc	0.50 ppm	0.4 ppm
Tin	0.01 ppm	0.01 ppm

2.4.3 Conclusions

(a) Decreasing the tin percentage of lead/tin solders increases the corrosion rate.

(b) The corrosion rate of the lead/tin solders was increased by bimetallic contact with the brass washer.

(c) The brass washers in all cases were highly resistant to corrosion, suffering no surface attack.

(d) Chemical analysis of the test solutions (Table 6) shows that lead is preferentially attacked in the solder.

2.5 The Effect Of Lead Ions In Solution On The Corrosion Of Aluminium

2.5.1 Trial Conditions

The conditions for this experiment were as described in the previous section, with aluminium and lead immersed in one beaker separated by a plastic washer and aluminium on its own in a second beaker. The 50% ethanediol solutions were kept at a constant 85°C for ten days with a cooling period of two hours per day, the change in weight was determined and the corrosion rate per day calculated.

2.5.2 Results

The results are given in Table 7 below.

Table 7

Beaker Number	Solution	Metals	Weight Loss Rate Over The 10 Day Period
1	50% Ethanediol Solution	Lead	8.5 mg $cm^{-2}d^{-1}$
		Aluminium	0.08 mg $cm^{-2}d^{-1}$
2	50% Ethanediol Solution	Aluminium	+ 0.2 mg $cm^{-2}d^{-1}$

Aluminium had not lost much weight in the presence of lead due to the deposition of lead on the aluminium surface. The aluminium had suffered localized corrosion and had been perforated. When on its own the aluminium did not corrode.

The experiment was repeated with an LTS/Brass Joint combination and aluminium in the same solution but not connected. It has been

shown in section 2.4 that the corrosion rate of lead tin solders is increased by bimetallic contact with brass. Since it is the lead from the LTS Solder which goes into solution, this would be expected to have an adverse effect on the corrosion of aluminium. The results of this experiment are given in Table 8 below.

Table 8

Beaker Number	Solution	Metals	Weight Loss Rate Over The 10 Day Period
3	50% Ethanediol Solution	LTS Solder/ Brass Joint	10.7 mg $cm^{-2}d^{-1}$
		Aluminium	0.2 mg $cm^{-2}d^{-1}$

The aluminium was again perforated.

2.5.3 Conclusions

Aluminium does not corrode when exposed to 50% ethanediol on its own, but when it is exposed in combination with lead or lead alloys, localized pitting corrosion takes place. Any galvanic effect which enhances the rate of corrosion of the lead tin alloys, also increases the corrosion rate of aluminium exposed to the same electrolyte.

2.6 Investigation To Isolate The Cations And Anions Which Play An Active Role In The Initiation Of Pitting Of Aluminium Samples Exposed To 50% Ethanediol/Tap Water Solution In The Presence Of Lead/Tin Alloys

Aluminium samples placed into 50% ethanediol/tap water test solutions along with lead/tin alloy test samples (these metal test samples not being in electrical contact) become coated with a crystalline deposit of lead metal. This is due to lead cations, a product of the corrosion of the lead/tin alloy samples, plating out onto the aluminium metal surface. These coated aluminium samples developed pits and pin holes, due to lead/aluminium bimetallic cells being set up on the aluminium's surface. Bohni and Uhlig [17], and Davies [64], have shown that copper cations plating out on aluminium stimulate and enhance the rate of localized corrosion of aluminium. It is likely, therefore, that the deposition of lead metal on to the aluminium surface plays a part in the overall corrosion mechanism; but other anions and cations introduced into the test solution as hardness salts in the make-up water must also be involved.

Tap water in all areas contains soluble salts, the main ones being calcium and magnesium chloride, calcium and magnesium carbonate and calcium and magnesium sulphate.

The aim of the following experiments is to determine whether or not soluble salts do play any part in the overall corrosion mechanism of aluminium.

The test rig was as described in section 2.4 with four automobile solders

(LTS, LTS P, 15% and 30% solder) and aluminium threaded onto a glass rod and held in position and separated with plastic washers. Each specimen was 2.5 cm square and was weighed before the experiment commenced. One test rig was placed in 250 mls of 50% ethanediol in double distilled water and the other in 250 mls of 50% ethanediol in tap water.

2.6.1 Trial Conditions

The solutions were kept in an oven at a constant 85°C. The oven was switched off each day for two hours to simulate engine stop periods and cold starts. The trial period was for fifteen days and during this time regular examination of the metal samples was carried out. At the end of the trial period, the metal samples were removed from the ethanediol solutions and cleaned. All the metal samples were then dried and re-weighed. The rates of corrosion were then calculated. These results are given in Table 9.

2.6.2 Conclusions

The increase in weight of the aluminium sample in 50% ethanediol/ double distilled water solution is due to the deposition of lead metal on the aluminium surface. Although lead was deposited on both aluminium samples, the only one which developed pits was the aluminium in ethanediol/tap water solution. This indicates that hardness salts as well as heavy metal cations in solution are necessary for pitting to occur.

Result Table 9

Corrosion Rates Of Automobile Solders And Aluminium In 50% Ethanediol Solution With And Without Hardness Salts

Solution	Metals	Rate Of Area Weight Loss Over Trial Period Of Fifteen Days
1 - 50% Ethanediol Double Distilled Water	LTS Solder	2.19 mg $cm^{-2}d^{-1}$
	LTS P Solder	2.09 mg $cm^{-2}d^{-1}$
	15% Tin Solder	0.90 mg $cm^{-2}d^{-1}$
	30% Tin Solder	0.40 mg $cm^{-2}d^{-1}$
	Aluminium	+ 0.010 mg $cm^{-2}d^{-1}$
2 - 50% Ethanediol Tap Water	LTS Solder	1.08 mg $cm^{-2}d^{-1}$
	LTS P Solder	1.65 mg $cm^{-2}d^{-1}$
	15% Tin Solder	0.30 mg $cm^{-2}d^{-1}$
	30% Tin Solder	0.09 mg $cm^{-2}d^{-1}$
	Aluminium	0.010 mg $cm^{-2}d^{-1}$

In order to identify the salt responsible for the pitting of aluminium, the experiment was repeated with 30 ppm of various salts in 50% ethanediol double distilled water. The salts were calcium chloride, calcium sulphate, magnesium chloride, magnesium sulphate and sodium carbonate. Any change taking place on the aluminium surface was noted. The results are given in Table 10.

It is concluded that pitting occurs when 30 ppm of chloride anions are present in solution together with heavy metal cations. In the absence of the heavy metal cations, pitting would not occur in a solution of 30 ppm chloride. The maximum concentration of chloride in tap water is usually 25 ppm, and, therefore, aluminium would be stable in a 50% ethanediol solution made up using tap water which was free from heavy metal cations. Carbonate and sulphate anions did not initiate localized corrosion of aluminium, even in the presence of heavy metal cations.

2.6. Discussion

Since the lead/tin alloy is not in contact with the aluminium, the pitting could not have been stimulated by direct galvanic effect. The pitting corrosion of aluminium must, therefore, be initiated by lead or tin cations or both, which have been released into the ethanediol solution from the lead/tin alloy, depositing on the aluminium. In order to determine whether it is the lead or tin which is responsible for the pitting, the aluminium was immersed in separate solutions of 50% ethanediol/double distilled water containing 50 ppm of stannous chloride, lead chloride, lead nitrate and potassium chloride. The condition being similar to the preceeding experiments at 85°C. The aluminium sample did not develop pits in stannous chloride, lead nitrate or potassium chloride containing solutions. Pits only developed on the aluminium samples exposed to lead chloride solution. These results show that both lead cations and chloride anions must be present for pit formation.

Results Table 10

Corrosion Rate Of Automobile Solders and Aluminium In 50% Ethanediol Solution Containing Various Hardness Salts

Hardness Salts	Metal	Rate Of Area Weight Loss Over Trial Period Of Fourteen Days	Observations
Calcium Chloride	LTS	1.57 mg $cm^{-2}d^{-1}$	Pinholes developed on the aluminium and increased in size with time.
	LTS P	1.78 mg $cm^{-2}d^{-1}$	
	15% Tin Solder	0.60 mg $cm^{-2}d^{-1}$	
	30% Tin Solder	0.48 mg $cm^{-2}d^{-1}$	
	Aluminium	0.08 mg $cm^{-2}d^{-1}$	
Calcium Sulphate	LTS	1.62 mg $cm^{-2}d^{-1}$	No pits developed on the aluminium.
	LTS P	1.89 mg $cm^{-2}d^{-1}$	
	15% Tin Solder	0.50 mg $cm^{-2}d^{-1}$	
	30% Tin Solder	0.003 mg $cm^{-2}d^{-1}$	
	Aluminium	0.0004 mg $cm^{-2}d^{-1}$	
Magnesium Chloride	LTS	1.23 mg $cm^{-2}d^{-1}$	Four large holes developed on the aluminium.
	LTS P	1.37 mg $cm^{-2}d^{-1}$	
	15% Tin Solder	0.64 mg $cm^{-2}d^{-1}$	
	30% Tin Solder	0.76 mg $cm^{-2}d^{-1}$	
	Aluminium	0.10 mg $cm^{-2}d^{-1}$	
Magnesium Sulphate	LTS	0.60 mg $cm^{-2}d^{-1}$	No pits developed on the aluminium.
	LTS P	0.57 mg $cm^{-2}d^{-1}$	
	15% Tin Solder	0.007 mg $cm^{-2}d^{-1}$	
	30% Tin Solder	+ 0.07 mg $cm^{-2}d^{-1}$	
	Aluminium	+ 0.009 mg $cm^{-2}d^{-1}$	

Hardness Salts	Metal	Rate Of Area Weight Loss Over Trial Period Of Fourteen Days		Observations
Sodium Carbonate	LTS	0.90	mg $cm^{-2}d^{-1}$	No pits
	LTS P	0.801	mg $cm^{-2}d^{-1}$	developed
	15% Tin Solder	0.08	mg $cm^{-2}d^{-1}$	on the
	30% Tin Solder	+ 0.12	mg $cm^{-2}d^{-1}$	aluminium.
	Aluminium	+ 0.016	mg $cm^{-2}d^{-1}$	
Blank - No Hardness Salts	LTS	2.47	mg $cm^{-2}d^{-1}$	No pits
	LTS P	2.16	mg $cm^{-2}d^{-1}$	developed
	15% Tin Solder	0.89	mg $cm^{-2}d^{-1}$	on the
	30% Tin Solder	+ 0.08	mg $cm^{-2}d^{-1}$	aluminium.
	Aluminium	+ 0.01	mg $cm^{-2}d^{-1}$	

2.7 The Effect Of Varying The Ethanediol Concentration Of A Tap Water Solution On The Corrosion Rate Of Lead Tin Solder Alloys Normally Found In An Automobile Cooling System

It is recommended that the engine coolant should contain fifty percent by volume of ethanediol. However, it is possible for the concentration to fall below this value since tap water is often added to top-up the level of coolant in the radiator to compensate for leakage.

Solders, especially low tin solders, suffer general surface attack when exposed to solutions of ethanediol, releasing lead cations (Pb^{2+}) into solution. These cations plate out on other metals in contact with the coolant. In the case of aluminium, this is particularly detrimental since it causes localized corrosion.

The conditions of the experiment are as described in section 2.4, with the four solders LTS, LTS P, 15% tin and 30% tin threaded onto a glass rod and separated with plastic washers. Each specimen was 2.5 cm square.

Four rigs were prepared for the four concentrations of ethanediol investigated, namely 0%, 5%, 25% and 50%.

2.7.1 Experimental Conditions

The four beakers containing 250 mls of test solution were placed in a thermostatically controlled oven at 85°C for twenty days. The oven was switched off for two hours each day to simulate engine stop periods and cold starts, the volume of the test solutions was kept constant by the addition of tap water.

At the end of the trial period, the solder samples were cleaned and the loss in weight determined. The corrosion rates were then calculated and the results are given in Table 11.

2.7.2 Conclusions

(a) The corrosion rate of solder increases as the ethanediol concentration increases from 15% to 50%. The corrosion rate in tap water is similar to that in 50% ethanediol.

(b) The corrosion rate in all solutions decreases as the tin content of the alloy increases.

Results Table 11

Corrosion Rates Of Automobile Solders In Ethanediol Solutions Of Various Concentrations

Solution Percentage	Solder	Rate Of Area Weight Loss Over Trial Period Of Twenty Days	
Tap Water -	LTS	0.81	mg cm^2d^{-1}
0% Ethanediol	LTS P	1.43	mg cm^2d^{-1}
	15% Tin	0.18	mg cm^2d^{-1}
	30% Tin	0.05	mg cm^2d^{-1}
15% Ethanediol	LTS	0.44	mg cm^2d^{-1}
	LTS P	0.35	mg cm^2d^{-1}
	15% Tin	0.06	mg cm^2d^{-1}
	30% Tin	0.01	mg cm^2d^{-1}
25% Ethanediol	LTS	0.60	mg cm^2d^{-1}
	LTS P	1.14	mg cm^2d^{-1}
	15% Tin	0.12	mg cm^2d^{-1}
	30% Tin	0.06	mg cm^2d^{-1}
50% Ethanediol	LTS	1.07	mg cm^2d^{-1}
	LTS P	1.51	mg cm^2d^{-1}
	15% Tin	0.19	mg cm^2d^{-1}
	30% Tin	0.04	mg cm^2d^{-1}

2.8 Investigation Of Lead Deposition On Aluminium Test Samples Exposed To Lead Chloride Test Solution, Using A Jeol 35C Scanning Electron Microprobe.

From the preceding experimental work it has been shown that aluminium when exposed to double distilled water or 50% ethanediol containing lead chloride, develops pits after a short period of time. Analysis of deposits on the pitted aluminium surface show that lead metal has plated out onto the surface as part of the overall pitting corrosion mechanism.

The aim of this experimental work is to determine:-

(i) Whether the lead metal is deposited before, after or during pit initiation.

(ii) The distribution of the lead metal around the formed pit.

2.8.1 Experiment

A sheet of the aluminium test foil was sectioned off into squares 4 cm^2 and these were stamped with the numbers 1 - 20. The sheet was then degreased in acetone and dried. A solution of 200 ppm lead chloride (AnalaR grade) in double distilled water was prepared and a drop (approximately 1 ml) of this solution was placed on the centre of each square. These drops of lead chloride solution were allowed to stand on the aluminium sheet for varying lengths of time.

Square 1 was exposed to the corrosive solution for 10 seconds. Square 2 was exposed to the solution for 30 seconds and each other square

was then exposed to the solution in increments of 20 seconds extra. Square 19 was exposed for 370 seconds. Square 20 was not exposed to the solution and can be considered the blank or control.

Extensive pitting corrosion had developed by square 6, hence squares 1 - 6 should contain the intermediate development stages of the pitting corrosion mechanism. Squares 1 - 6 were therefore cut out. The circular central exposed area of each square was mounted and carbon coated and examined using the scanning electron microscope microprobe (Jeol 35C).

2.8.2 Results

Examination of squares 1 - 4 (10 seconds - 70 seconds exposure) showed no crystalline deposits of lead and no signs of pit development were observed. Electron microprobe analysis did not detect any lead on the surface of the aluminium samples.

Figure 10 is a photograph of sample 5 clearly showing a pit surrounded and partially covered by white crystalline material, which when analysed using the electron microprobe, was found to contain a high percentage of lead. Lead was also detected on the rest of the aluminium surface.

Figure 11 is a lead fluorescence photograph of Figure 10. All light areas contain a high percentage of lead. Therefore it can be readily seen that all the crystalline structures surrounding the pit stand out well in the fluorescence photograph, confirming that they do contain a high percentage of lead.

Figure 13 shows that the surface film is much thicker around and over the pit. This thickening is not due to lead deposition.

2.8.3 Conclusions

Aluminium samples treated in lead chloride solution did not have any detectable surface deposit of lead for the first seventy seconds of exposure. After this time a lead deposit on the exposed surface was detected and pits became visible almost simultaneously.

The first seventy seconds of the pitting corrosion reaction in lead chloride containing solutions of either double distilled water or 50% ethanediol, can, therefore, be looked on as an induction period, when halide anions penetrate or interact with the alumina film.

It may be seen from Figure 13 that fully developed pits were seen to have a thick cracked film over and around the pit mouth, fine cracks radiating out into the thickened surface film around the pitted area.

The electrons released during aluminium cation formation, equation 7:-

$$Al = Al^{3+} + 3e^{-} \qquad (7)$$

react with the free lead cations near the aluminium surface solution boundary, forming lead metal, equation 8:-

$$Pb^{2+} + 2e^{-} = Pb\ (Metal) \qquad (8)$$

The aluminium cations are hydrolysed as in equation 9, this causes the thickening of the film in the vicinity of the pit. Figure 13.

$$2\,Al^{3+} + 6H_2O = 2Al(OH)_3 + 3H_2 \qquad (9)$$

Earlier work has shown that lead cations as well as chloride anions have to be present in solution for localized corrosion of aluminium to take place. It has also been established that on exposure of aluminium to lead halide solutions, no lead is deposited on the aluminium for the first 60 seconds. Therefore, assuming that initiation of localized corrosion of the aluminium takes place immediately that the sample is placed in the lead halide solution, it cannot be the presence of galvanic cells set up by deposited lead that initiates pitting of the aluminium, but the lead cations in solution.

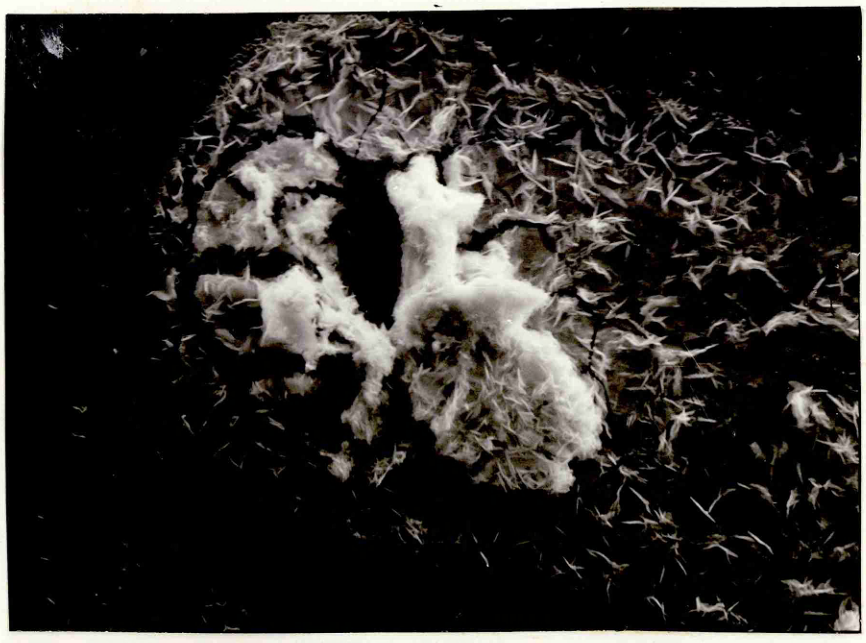

Figure 10 Photograph Of A Partially Covered Pit, Which Had Developed On Aluminium On Exposure To Lead Chloride Solution

Figure 11 Lead Fluorescence Photograph Of The Same Area Illustrated In Figure 10

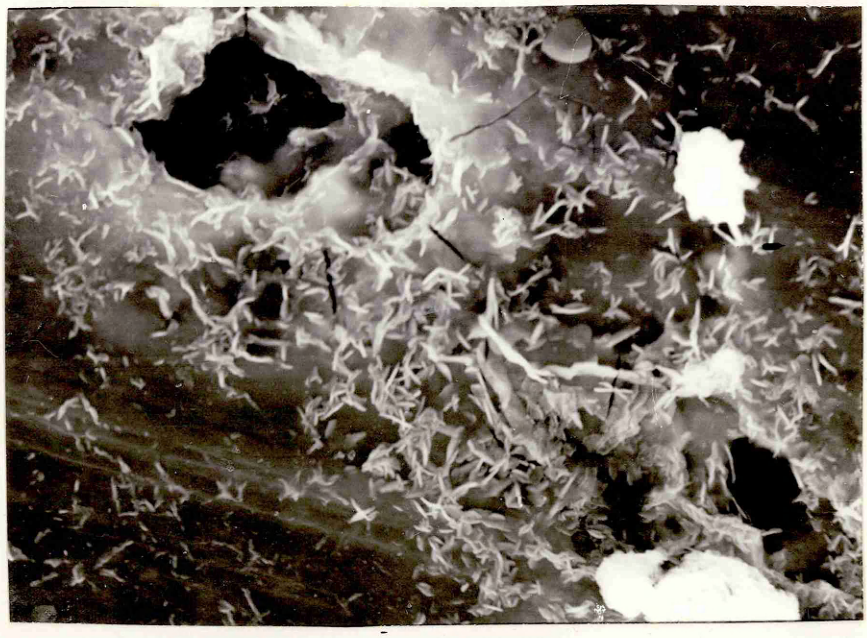

Figure 12 Photograph Of Two Open Pits Surrounded By A Cracked Surface Film, Which Developed On Aluminium Exposed To Lead Chloride Solution

Figure 13 Photograph Of The Cracked Thickened Surface Film Surrounding A Pit, Which Developed On Aluminium Exposed To Lead Chloride Solution

CHAPTER 3

3.0 Determination Of The Critical Pitting Potential, Ep, Of Aluminium In Solutions Containing Fluoride, Chloride, Bromide Or Iodide

3.1 Introduction

Pits form at potentials more positive than a certain critical value known as the critical pitting potential.

This can be demonstrated by electrochemical measurements using potentiostatic techniques and Figure 14 represents a typical curve. In the absence of halide ions, A, B, C, D, E represents the usual polarization behaviour, but when conditions suitable for pitting prevail, there is a sudden increase of current, represented by FG, in the passive region accompanied by pitting.

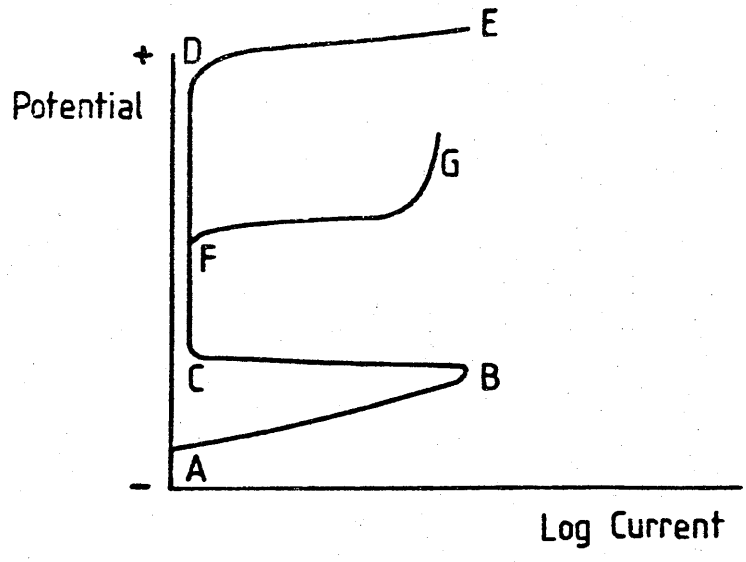

Figure 14 Typical Anodic Polarization Potential Curve, Produced Using A Potentiostatic Technique

The point of departure from the passive region F is referred to as the critical pitting potential, but it is time dependent.

Aluminium metal used to construct heat exchangers or engine blocks can be exposed to ethanediol containing coolant contaminated with fluoride, chloride and bromide anions. The experimental work to be described is designed to determine the critical pitting potential of aluminium samples placed in solution of these halide anions in 50% ethanediol/double distilled water and in double distilled water.

From a theoretical point of view, as the size of the halide anions increase from fluoride to iodide, Table 12, the Ep value would be expected to increase in nobility in the same order. Hoar, Mears and Rothwell [8], found that chloride ions were more aggressive than bromide and iodide anions, in that order which would seem to confirm this theory.

Table 12

Ionic Radii Of Halide Anions

Halide	Ionic Radius
F^-	1.36×10^{-10} m
Cl^-	1.81×10^{-10} m
Br^-	1.95×10^{-10} m
I^-	2.16×10^{-10} m

The temperature and halide concentration of the coolant to which aluminium can be exposed will also vary. Cocks [65], has shown that pitting potential Ep became more negative as the chloride ion concentration increased and also with increasing temperature. Bohni and Uhlig [17],

and also De Micheli [66], also observed similar changes in Ep with increase of chloride concentration in double distilled water.

3.2 Experiment

A schematic diagram of the apparatus is shown in Figure 15. The Luggin probe could be moved towards the working electrode and in order to prevent I.R. drop, the tip was arranged to be about 0.5 mm from the surface of the working electrode.

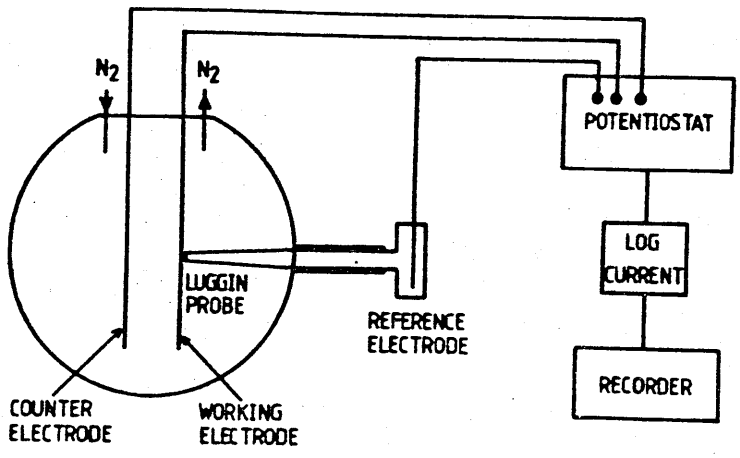

Figure 15 Schematic Diagram Of Apparatus For Critical Pitting Potential Determination

A Wenking PGS 81 potentio-galvano scan was used in the investigation and the current was recorded logarithmically with time. The corrosion cell was constructed from polypropylene because of a possible glass-sodium fluoride interaction. The counter electrode was platinised titanium and a mercury/mercurous sulphate reference electrode was used in order to avoid chloride contamination. The four halide salts selected for this work, sodium fluoride, potassium chloride, potassium

bromide and potassium iodide, and all other chemical reagents used including the ethanediol, were of AnalaR grade.

The working electrodes were made from aluminium in the form of foil 100 μm thick, whose composition is given in section 2.2. The foil was cut into strips 1 cm wide and 15 cm long, which were then degreased in acetone and dried under a hot air blower. Lacomit lacquer was then painted onto the surface, leaving an exposed active rectangular area of 1.5 cm x 1.0 cm for contact with the end of the Luggin probe, and an area of 1.0 cm x 1.0 cm at the end for contact with the working electrode output of the potentio-galvano scan. The prepared samples were all examined using a stereoscopic microscope at a magnification of 40X for surface defects, i.e. deep scratches or marks that could be confused with pits. All samples with surface defects were rejected.

The water used in all solutions was double distilled deionised water. Solutions of concentrations 25 ppm, 50 ppm, 75 ppm, 100 ppm and 125 ppm by weight were made up for each of the four halide salts in both double distilled water and 50% ethanediol double distilled water, forty test stock solutions in all.

The pitting potential (Ep) in relation to this research project is defined as the most negative or least noble potential at which pitting actually occurs on every sample tested. From past experimental work, three criteria can effectively be used to evaluate whether pitting has actually occurred:-

(i) large rapid rise in current at a fixed constant potential;

(ii) appearance of air bubbles being exuded from the aluminium surface, a method which can only effectively be used at low temperatures 25°C ± 5°C.

(iii) observation of pits on the sample.

The test solution under investigation was first de-oxygenated by passing fine bubbles of white spot grade (oxygen free) nitrogen through the test solution for fiteen minutes. This time period was determined by bubbling de-oxygenated nitrogen through test solutions, and removing samples at frequent time intervals. The soluble oxygen concentration was then determined by the Winkler method, and hence the optimum de-oxygenation period determined.

The test specimen was then placed in the working electrode clamp and lowered into the test solution until the exposed surface was opposite the end of the Luggin probe. A slight back-pressure of nitrogen was maintained inside the corrosion cell in order to prevent oxygen diffusing in, and dissolving in the test solution.

The initial trials were concentrated on the eight stock solutions which contained the 100 ppm by weight concentration of halide. A potentio-dynamic polarization curve was determined for the aluminium in each de-oxygenated stock solution over the range 0 to - 1.0 volt, at a rate of 2 mV/sec., current being recorded continuously on an X/Y model recorder. The pitting potential is time dependent and, therefore, the values obtained in this manner are only approximate.

In order to obtain an accurate pitting potential a potentio-static technique was used in which the aluminium sample was held at the appropriate approximate pitting potential for a period of twenty hours, and the sample graded as either pitted or not. If the former is the case, the potential was then made more cathodic by -20 mV and a freshly prepared specimen was exposed for the same period of time. This procedure was repeated until the sample did not pit, in this case the potential was then made more noble by -10 mV and a fresh sample exposed for the set period. Thus the pitting potential could be determined within an accuracy of $\pm$ 5 mV.

It should also be noted that at potentials near the Ep figure, the third criterion only was used to evaluate whether or not pitting had taken place.

The solution temperature was maintained at 25°C $\pm$ 1°C in all cases, using a thermostatically controlled heating mantle. However, in order to evaluate the effect of increasing temperature on pitting potential, potentio-static corrosion trials were also carried out at 50°C and 75°C in solutions containing 50 ppm by weight for each of the halide salts.

3.3 Results

The pitting potentials of aluminium in the various solutions are given in Table 13, and the effect of temperature on Ep values is given in Table 14.

The values given are with reference to mercurous sulphate/sodium sulphate reference electrode, and are within an accuracy $\pm$ 5 mV.

This accuracy was achieved by determining in the first instance the potentiodynamic curve, a typical curve for 50 ppm KCl in double distilled water is shown in Figure 25. This gives an approximate pitting potential of - 0.80V, the experiment was then repeated potentio-statically at this potential and the curve obtained is shown in Figure 26. The set potential was then made more negative by 20 mV, and the potentio-static curve again determined. This procedure was repeated until a potential was found which gave a trace similar to that in Figure 27 and no pitting took place. The potential was then made more positive in steps of 10 mV until a curve similar to that in Figure 26 was obtained, indicating breakdown. This potential was then recorded as the critical pitting potential. The curves obtained for other concentrations of chloride were similar and also the curves for bromide and iodide.

The potentiodynamic polarization curve for aluminium in 50 ppm by weight sodium fluoride in double distilled water did not reveal a well defined breakdown potential, Figure 28. Surface activity typical of localized corrosion was visible at - 0.50V, and the small increase in current at approximately - 0.0V does not have any significance in that it occurred at other potentials in repeat experiments.

Again the potentiostatic curve for the fluoride solution did not indicate the breakdown potential. The potentiostatic trace in Figure 29 is typical of the current variation above and below the pitting potential, the only way of establishing pitting potential in fluoride solution was by visual observations.

Results Table 13

Effect Of Halide Concentration On The Pitting Potential Of Aluminium

Halide and Conc. In ppm	Ep In Double Distilled Water	Ep In 50% Ethanediol Double Distilled Water
25 ppm NaF	- 0.49V	- 0.44V
50 ppm NaF	- 0.52V	- 0.46V
75 ppm NaF	- 0.55V	- 0.52V
100 ppm NaF	- 0.59V	- 0.55V
125 ppm NaF	- 0.59V	- 0.57V
25 ppm KCl	- 0.85V	- 0.84V
50 ppm KCl	- 0.88V	- 0.86V
75 ppm KCl	- 0.91V	- 0.88V
100 ppm KCl	- 0.91V	- 0.89V
125 ppm KCl	- 0.92V	- 0.90V
25 ppm KBr	- 0.70V	- 0.71V
50 ppm KBr	- 0.72V	- 0.73V
75 ppm KBr	- 0.75V	- 0.73V
100 ppm KBr	- 0.77V	- 0.74V
125 ppm KBr	- 0.78V	- 0.76V
25 ppm KI	- 0.57V	- 0.55V
50 ppm KI	- 0.57V	- 0.55V
75 ppm KI	- 0.58V	- 0.55V
100 ppm KI	- 0.58V	- 0.55V
125 ppm KI	- 0.58V	- 0.55V

Results Table 14

Effect Of Temperature On The Pitting Potential Of Aluminium

Alkaline Metal Halide Salt	Temperature	Ep In Double Distilled Water	Ep In 50% Ethanediol Double Distilled Water
50 ppm by weight Potassium Chloride	25°C	- 0.88V	- 0.86V
	50°C	- 0.96V	- 0.88V
	75°C	- 1.00V	- 0.91V
50 ppm by weight Potassium Bromide	25°C	- 0.72V	- 0.73V
	50°C	- 0.80V	- 0.74V
	75°C	- 0.84V	- 0.76V
50 ppm by weight Sodium Fluoride	25°C	- 0.52V	- 0.45V
	50°C	- 0.86V	- 0.85V
	75°C	- 1.00V	- 0.96V

3.4 Conclusions

The nobility of the critical pitting corrosion potential (Ep) of aluminium exposed to halide containing solutions of double distilled water and 50% ethanediol (Results Tables 13 and 14) decreases with increase in halide concentration and solution temperature in the range 25°C - 75°C. This is in agreement with the work carried out on chloride containing solutions by Cock [65], Bohni and Uhlig [17].

The Ep values for aluminium at similar halide concentrations in 50% ethanediol solution, compared with those for double distilled water were of slightly higher nobility.

Theoretically, if the penetration theory of pitting corrosion initiation is correct, the smaller the anion the easier it should penetrate the aluminium oxide passive layer. This should, therefore, be reflected in the Ep value, those for small anions e.g. fluoride, being less noble than those for larger anions e.g. iodide. From the Ep values for the various halide containing solutions, Table 13, fluoride seems to be out of sequence contradicting this theory.

The potentiodynamic and potentiostatic traces of aluminium exposed to sodium fluoride containing solutions, Figures 28 and 29, did not show the characteristic current oscillation and rapid rise in current which is attributed to the passive film breakdown and pitting initiation, this can be clearly seen in the chloride traces, Figures 25 and 26. This suggests that some other secondary reaction is taking place on the aluminium surface when it is exposed to fluoride containing solutions.

Dallek and Foley [67], found similar anomalies in their study of the

stability of aluminium halide complexes which are supposed to form in the adsorption pitting theory, and which accelerate hydration of the aluminium oxide film. They determined the order of reaction, (i.e. number of anions per aluminium surface reaction site) and the energy of activation for pitting initiation for aluminium samples exposed to solutions containing F^-, Cl^-, Br^- and I^- anions. The technique used was that developed by Hoar and Jacob [19] to measure the kinetics of breakdown of passive layers on iron and stainless steel by halide ions, later adapted for aluminium by Bogar and Foley [68], Foroulis and Thubrikar [69].

In this technique the metal electrode is held potentiostatically in the passive range in an appropriate electrolyte, a specific concentration of halide anions is injected into the electrolyte, and the induction time, t, for a sharp rise in current is recorded. The rapid rise in current is correlated with the breakdown of passivity and initiation of pitting.

From this induction time, it is possible to arrive at the order of the reaction, n, the number of halide ions associated with the dissolution of a single aluminium atom, and the energy of activation, Ea.

The reciprocal of the induction time determined from the current/time trace $^1/_t$, is taken as the rate of pit initiation, i.e. the number of events per unit time.

The rate equation is then:-

$$(^1/_t) = K\ [Al]^m\ [X^-]^n \qquad (10)$$

wherein K is the rate constant, [Al] is the aluminium atom concentration, $[X^-]$ is the halide ion concentration, and m and n are the respective orders of reaction. The activity coefficients are included in K.

The logarithm form of (10) is:-

$$\text{Log } (^1/_t) = \text{Log } K + m \text{ Log } [Al] + n \text{ Log } [X^-] \qquad (11)$$

Thus, if K and [Al] are taken as constant, then the plot of Log $(^1/_t)$ vs Log $[X^-]$ will give n, the order of reaction with respect to X^- ions.

The authors propose that the term m Log Al is only constant for a specific halide reaction and that m is equivalent to the number of atoms involved in a surface reaction site, i.e. the co-ordination number of the surface in the sense used by Laidler[70] and others in their development of the theory of absolute rate of surface reaction.

At constant halide concentration, $(^1/_t)$ will be proportional to the rate constant and

$$(^1/_t) = Ae^{-Ea/RT} \qquad (12)$$

Thus a conventional Arrhenius plot of Log $(^1/_t)$ vs the reciprocal of the temperature will yield the apparent activation energy for the initiation process.

Dallek and Foley concluded from their experimental results that the aluminium chloride, bromide and iodide complexes would be intermediates in a step-wise process that terminates eventually with the formation

of the hydrated oxide film of aluminium. The aluminium fluoride complexes on the other hand would be insoluble and stable. In their experimental work they also noticed that the fluoride current traces did not exhibit rapid oscillation, and instead of increasing exponentially, reached a plateau. This is associated with the formation of a stable compound on the aluminium surface.

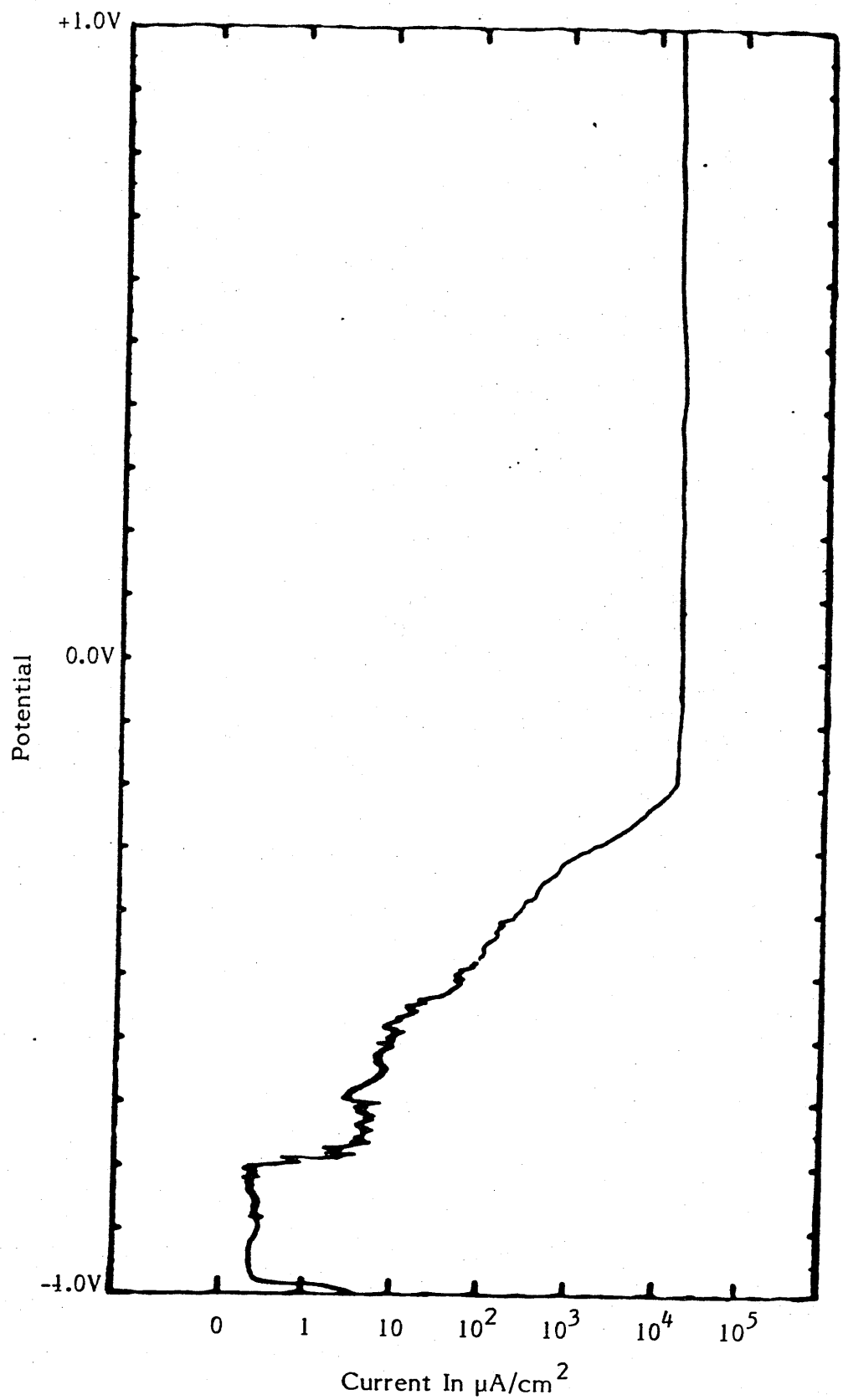

Figure 25 Potentiodynamic polarization plot of aluminium in 50 ppm by weight potassium chloride double distilled water solution.

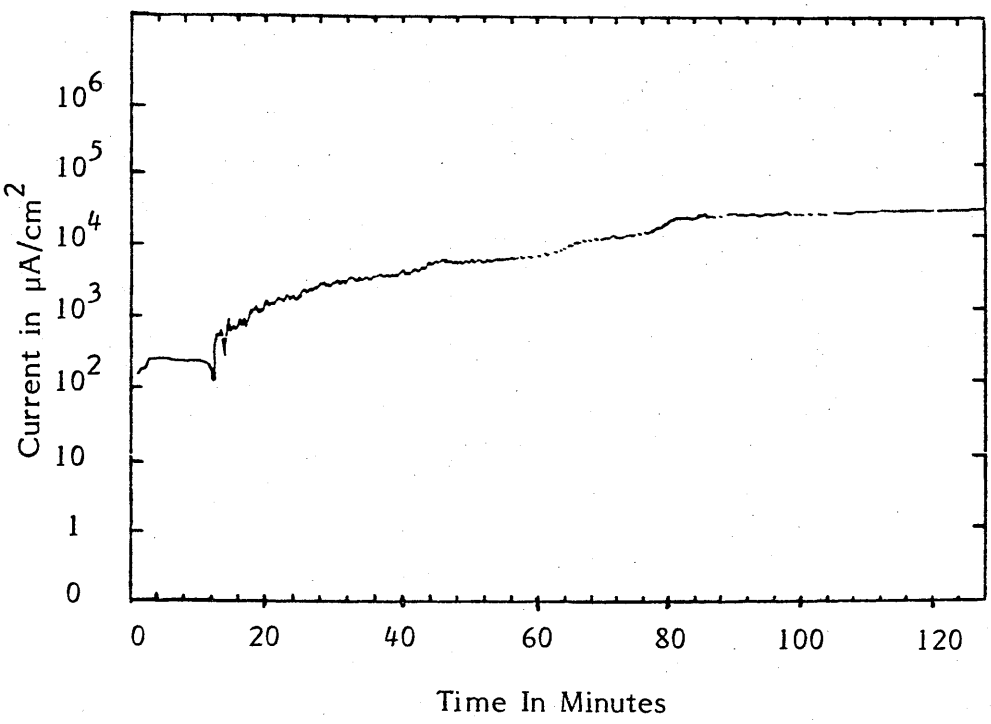

Figure 26 Potentiostatic trace of aluminium polarized to - 0.80V in 50 ppm by weight potassium chloride double distilled water solution.

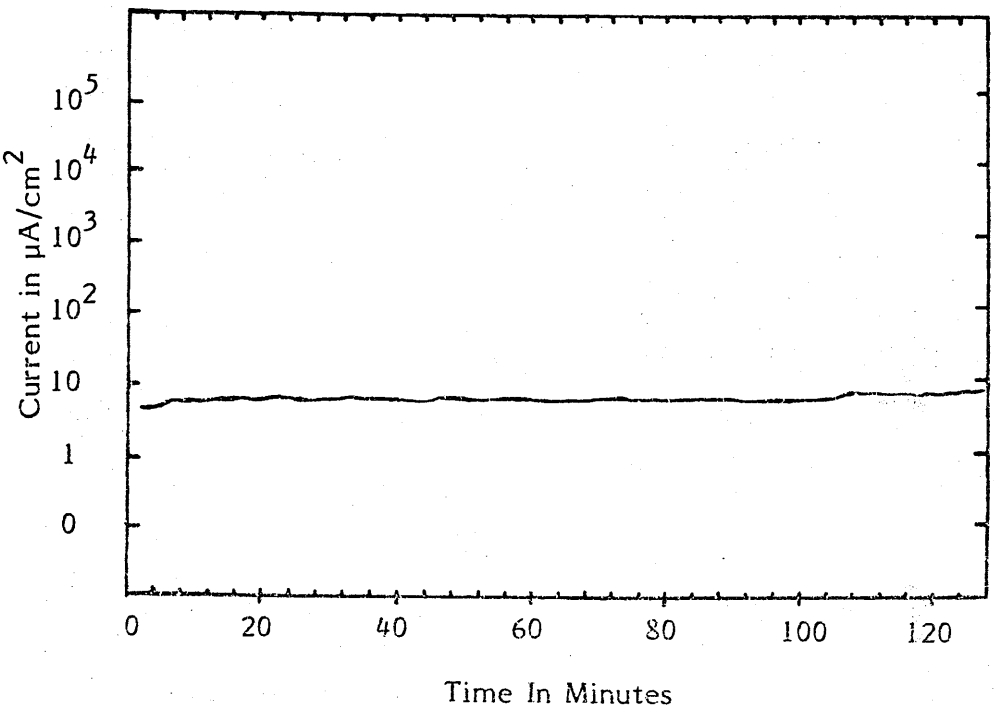

Figure 27 Graph of current against time of aluminium at a potential of - 0.89V in 50 ppm potassium chloride double distilled water solution.

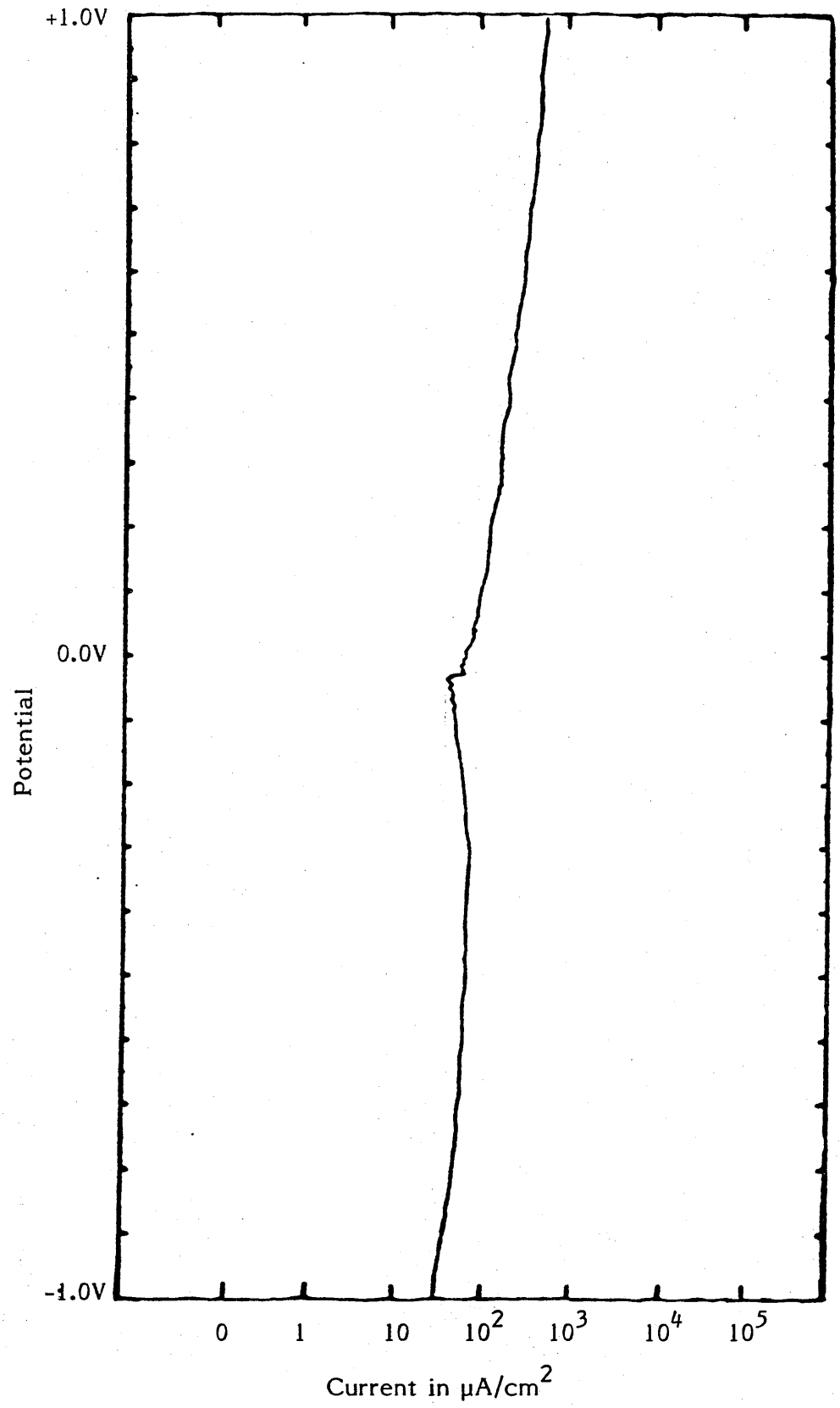

Figure 28 Potentiodynamic polarization of aluminium in 50 ppm by weight sodium fluoride double distilled water solution.

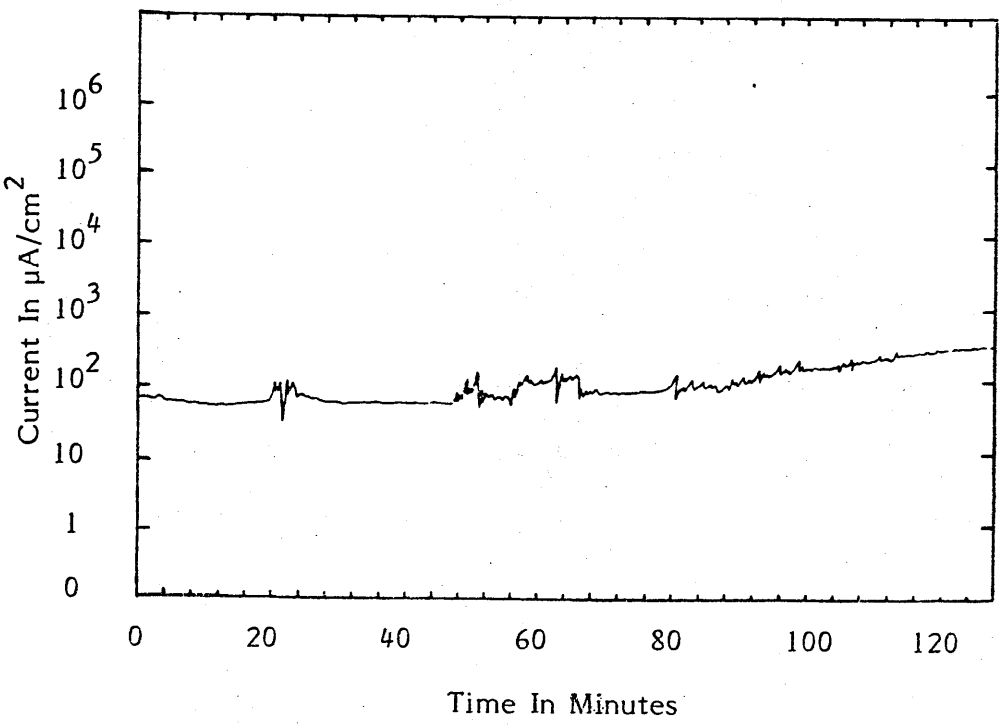

Figure 29 Potentiostatic trace of aluminium polarized to - 0.53V in 50 ppm by weight sodium fluoride double distilled water solution.

CHAPTER 4

4.0 The Effect Of Sodium Fluoride On The Localized Corrosion Of Aluminium In Deionised Water and 50% Ethanediol Solution.

4.1 Introduction

Since the size of the halide anions increases in the sequence fluoride, chloride, bromide and iodide (see Table 12), the critical pitting potential of an aluminium sample exposed to separate solutions of these halides would be expected to increase in nobility in the same order.

However, critical pitting potential evaluation experiments for these halides have shown that whilst this is the case for the chloride, bromide and iodide ions, the fluoride ion is out of sequence, the value of its critical pitting potential being as noble as that of the iodide ion (Table 13).

Similar results were obtained in solutions containing 50% ethanediol. The fluoride ion with the smallest ionic radius would be expected to be the most aggressive of the four halide ions and to cause serious pitting. However, from the critical pitting potential investigations, the fluoride ion has been found to be the least aggressive, both in double distilled and 50% ethanediol solutions.

Another difference between the fluoride and the other halides is in the current registered at the critical pitting potential. Whereas the chloride, bromide and iodide cause a sudden increase in current which after a period remains constant, as represented by FG in Figure 14, the current increase in the case of fluoride is very small and is only slightly greater than the passivation current FD. Pitting in the presence

of the fluoride ion is, therefore, not typical of the localized corrosion which takes place in the presence of chloride, bromide and iodide anions.

This behaviour suggests that a stable film forms on the aluminium surface in the presence of the fluoride ion which stifles the pitting at the expected critical pitting potential. However, the film cannot prevent pitting at all potentials and its effect is to move the critical pitting potential to a more noble value, close to that found for the iodide ion. The aim of the present experimental work is to investigate whether such a film forms and if so, the potential range in which it is stable.

4.1.1 Experiment

The apparatus and procedure were similar to those already described in section 3.2. A schematic diagram of the apparatus is shown in Figure 15. A mercury/mercurous sulphate/sodium sulphate standard E.I.L. reference electrode was used in order to avoid the possibility of chloride contamination from the calomel reference electrode. The counter electrode is platinised titanium.

The aluminium test samples were in the form of foil 100μm thick and had composition as given in section 2.2. The samples were cut into strips 10 cm long x 1 cm wide, each cut strip was degreased in acetone and dried under a hot air blower. Lacomit lacquer was then painted onto the surface, leaving a rectangular area 1.5 x 1.0 cm exposed to the Luggin probe. An area 1.0 x 1.0 cm was also left clear at the end of the sample for contact with the working electrode output of the potentio-galvano stat. The surface of the prepared samples was

examined for any defects using an optical microscope set at a magnification of 40X. All samples with deep scratches or pit-like structures were discarded.

A sodium fluoride concentration of 100 ppm by weight was selected for this experiment. Two stock solutions were made up, one of sodium fluoride in double distilled water, and the other of sodium fluoride in 50% ethanediol double distilled water.

Deaeration of the solution did not have an effect on the observed critical pitting potential, but since the oxygen content of the solution was determined before and after the experiment, nitrogen was passed over the solution in order to avoid oxygen pick up.

The potentio-static potentials of the separate aluminium samples in both test solutions were - 0.50V, - 0.55V, - 0.60V, - 0.65V, - 0.70V, - 0.75V, - 0.80V, - 0.85V, - 0.90V, - 0.95V and - 1.00V. The exposure period was twenty-four hours at each potential.

The test specimen was placed in the working electrode clamp and lowered into the test solution until the exposed surface was opposite the end of the Luggin probe. In order to prevent I.R. effects, the probe was brought up to the recommended distance of half the Luggin probe end orifice diameter away from the sample surface. The solution temperature was maintained at 25 $\pm$ 1°C.

The sample was removed and dried under a hot air blower. The surface was then examined under an optical microscope at a magnification

of between 20X to 50X for evidence of pitting and film formation.

A 200 ml sample of the test solution was taken before and after aluminium exposure for each test potential, for both double distilled and 50% ethanediol solutions. These samples were then subjected to various analytical techniques to determine:-

(i) soluble oxygen content of the solutions (Winkler method of analysis).

(ii) fluoride free soluble ions concentration. (Fluoride ion selective electrode connected to an E.I.L. model pH meter with ion selective electrode facility.)

Surface films formed were examined with the scanning electron microscope and microprobe analysis was also carried out.

4.1.2 Results

From the experimental observations, see Tables 15 and 16, and examination of the treated samples using the electron microscope/microprobe, it has been observed that a film forms on the aluminium in double distilled water containing 100 ppm sodium fluoride at potentials more negative than the critical pitting potential of - 0.59V. The thickness of this film, judging by its appearance, increased in thickness from - 0.6V to - 0.8V and then decreased to - 1.0V. In the 50% ethanediol solution containing 100 ppm sodium fluoride, the film which formed was thinner and remained the same from - 0.6V to - 0.8V. At potentials more negative than - 0.8V, the film was even thinner and resembled a tarnish

film in appearance (see Table 16).

Pit formation in double distilled water containing 100 ppm sodium fluoride at a potential of - 0.55V is seen in the scanning electron microscope photograph at a magnification of 300X, Figure 16.

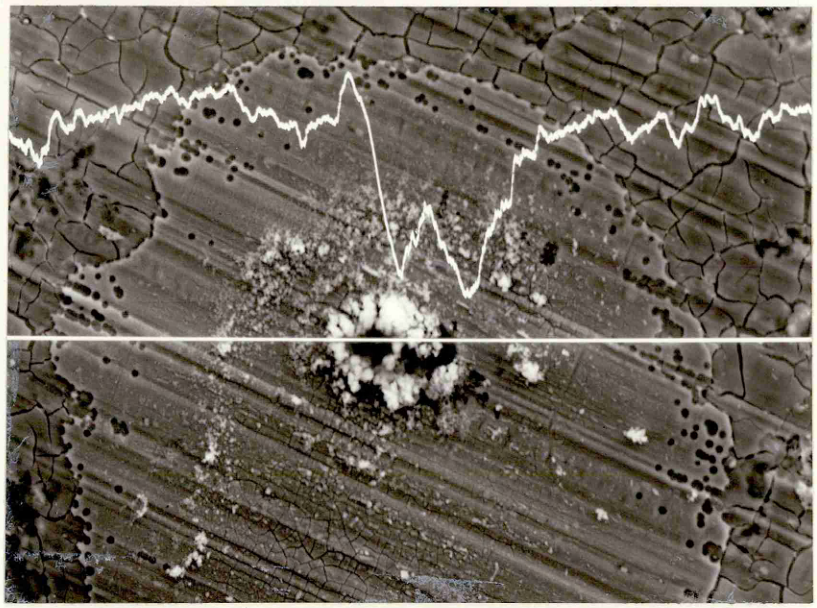

Figure 16 Pit Formed In Double Distilled Water Containing 100 ppm Sodium Fluoride At -0.55V Magnification 300X

It will be observed that the surface of the aluminium is covered with a fairly thick film. A fluoride trace and a horizontal base line have been superimposed on the photograph. The qualitative analysis shows a high concentration of fluoride in the film which decreases to a low value as it traverses the pit itself. It is apparent that exposed aluminium metal exists at the bottom of the pit which has developed as a result of the film breakdown.

The film itself formed at a potential when there is no breakdown (- 0.80V) is shown in Figure 17.

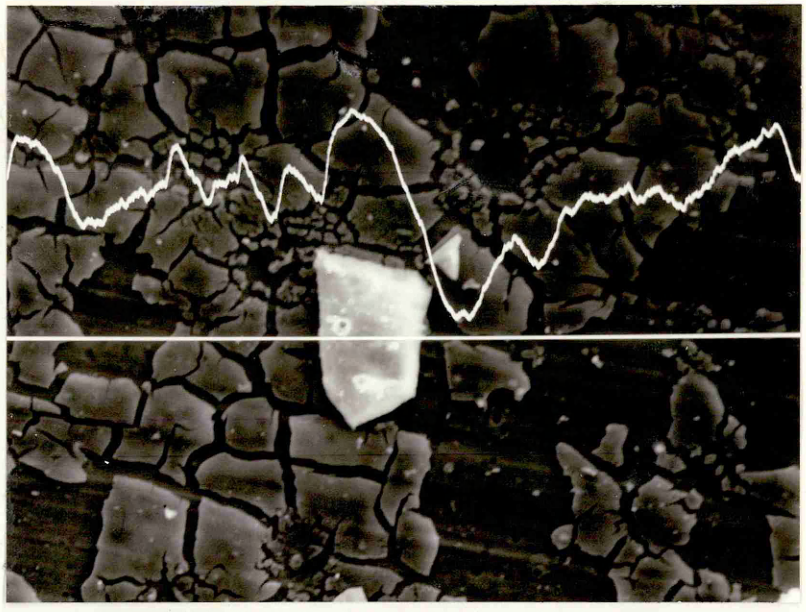

Figure 17 Film Formation In Double Distilled Water Containing 100 ppm Sodium Fluoride At -0.80V Magnification 300X

Three layers of film are observed, the outermost part represented by the large white area in the centre of the picture, a middle layer which shows extensive cracking and an adherent layer next to the metal. The microprobe trace shows that the film has fluoride content similar to that found when pitting took place as in Figure 16.

The film which forms at - 0.8V in 50% ethanediol containing 100 ppm sodium fluoride is shown in Figure 18 and is quite different from that seen with the scanning electron microscope in double distilled water at the same potential, Figure 17. The film is much thinner and the fluoride content is very low.

Figure 18 Film Formation In 50% Ethanediol Containing 100 ppm Sodium Fluoride At -0.80V

When specimens were held at a given potential for twenty-four hours in either double distilled water or ethanediol solution containing 100 ppm of sodium fluoride, there was a decrease in the fluoride content and the oxygen content of the solution, as shown in Table 17.

The rest potential of the aluminium was - 1.3V in double distilled water and 50% ethanediol solutions containing 100 ppm sodium fluoride. The current density at all potentials in the passive range was $0.1 mA/cm^2$ in double distilled water solutions and $0.01 mA/cm^2$ in 50% ethanediol.

Table 17 shows that the maximum decrease in oxygen content for double distilled water occurs at a potential of - 0.8V. Visual observations, Table 15, also indicates that the film is thickest at this potential.

Consequently the aluminium surface was examined after twenty-four hours at this potential, Figure 17.

The fluoride content of the film in the 50% ethanediol solution is fairly constant, but lower than in double distilled water, the maximum oxygen decrease occurring at a potential of - 0.7V.

4.1.3 Conclusions

(a) In the presence of fluoride a film forms on aluminium in double distilled water and 50% ethanediol at potentials more noble than - 1.0V vs mercury/mercurous sulphate reference electrode.

(b) The composition and the thickness of the film formed in double distilled water is different from that in 50% ethanediol when the fluoride ion is present. In the former, the film is much thicker and consists of three layers each having a different fluoride content, whilst the film formed in 50% ethanediol is thinner and has a much lower fluoride content.

(c) All the films formed contain fluoride and oxygen either as an oxide or hydroxide, but the relative amounts of oxygen and fluoride will vary depending on the set potential. The thickest film was found at a potential of - 0.8V in double distilled water and at a potential of - 0.70V in 50% ethanediol, but the passivation currents of 0.1mA/cm^2 observed in the former case and the 0.01mA/cm^2 registered in the 50% ethanediol, suggest that the film which forms in double distilled water is about ten times as thick as that which forms in the 50% ethanediol solution.

(d) Although the exact nature of the film is not known, it is probably some form of aluminium oxyfluoride or hydroxyfluoride.

Table 15

Observations On The Condition Of Aluminium Surface After Exposure At Various Potentials To Double Distilled Water 100 ppm Sodium Fluoride.

Potential Set Double Distilled Water + 100 ppm By Weight Sodium Fluoride	Observations
- 0.60V	Thick uniform surface film (buff in colour). Some sample edge attack.
- 0.70V	Thick uniform surface film (buff in colour).
- 0.80V	Thick uniform surface film (buff in colour).
- 0.90V	Light surface film (buff in colour), not totally uniform.
- 1.00V	Surface film (buff in colour), which appeared to be thicker than that formed at - 0.90V.

Table 16

Observations On The Condition Of Aluminium Surface After Exposure At Various Potentials To 50% Ethanediol 100 ppm Sodium Fluoride Solution.

Potential Set 50% Ethanediol + 100 ppm By Weight Sodium Fluoride	Observations
- 0.60V	Uniform surface film opaque/white. No signs of pit development.
- 0.70V	Surface film opaque/white, signs of surface attack.
- 0.80V	Surface film. Signs of surface attack.
- 0.90V and - 1.00V	Surface clear.

Table 17

Change In Fluoride And Soluble Oxygen Concentration Of 100 ppm By Weight Sodium Fluoride Double Distilled Water And 50% Ethanediol Solution After 24 Hours Exposure To Aluminium Samples At Various Set Potentials.

Potential Set	Double Distilled Water + 100 ppm By Weight Sodium Fluoride	Fluoride Concentration Change	Soluble Oxygen Change
- 0.60V		0.00018M	2.4 mg/l
- 0.70V		0.00020M	2.72 mg/l
- 0.80V		0.00022M	7.36 mg/l
- 0.90V		0.00030M	0.32 mg/l
- 1.00V		0.00030M	3.2 mg/l

Potential Set	50% Ethanediol + 100 ppm By Weight Sodium Fluoride	Fluoride Concentration Change	Soluble Oxygen Change
- 0.60V		0.00012M	3.80 mg/l
- 0.70V		0.00010M	4.64 mg/l
- 0.80V		0.00007M	3.20 mg/l
- 0.90V		0.00010M	0.96 mg/l
- 1.00V		0.0000 M	0.48 mg/l

4.2 Investigation To Determine Whether Fluoride Films Formed On Aluminium Samples Delay Pitting Corrosion

4.2.1 Introduction

It has been established that a film forms on aluminium when it is exposed potentiostatically to distilled water containing 100 ppm of sodium fluoride at potentials more negative than the critical pitting potential. The same applies to 50% ethanediol solutions containing 100 ppm of sodium fluoride. Film formation in fluoride solution has also been reported by Lorking and Mayne[71], who observed a white tenacious film of corrosion product at the rest potential in fluoride solution more concentrated than the one used in the present investigation. This film does not form in the absence of fluoride, neither does it form when chloride, bromide or iodide are present in solution.

It is suggested that this film is responsible for the more noble critical pitting potential observed for aluminium, both in distilled water and 50% ethanediol solution when the fluoride ion is present. The aim of this experiment is to determine whether this fluoride containing film does delay the pitting of aluminium.

4.2.2 Experiment

The standard equipment illustrated in Figure 10 and described in section 3.2 was used.

The experimental procedure was as described in the previous chapter.

Three potentials - 0.75V, - 0.80V and - 0.85V were selected from the - 0.75V to - 0.85V potential range as the potentiostatic treatment

potentials.

The potential was then set at one of the three selected potentials, and the sample was held at this potential for twenty-four hours. It was then dried and labelled with the treatment potential and solution. This procedure was then repeated until six samples had been treated for each of the three treatment potentials in both solutions, thirty-six samples in total.

The surfaces of the treated samples were then examined using an optical microscope with zoom magnification in the range 10X to 50X.

The protective properties or the ability of the film formed to delay the pitting process was then evaluated by exposing some of the treated samples to a chloride solution at a potential of - 0.85V where pitting is known to occur, the critical pitting potential being - 0.91V.

A solution of 100 ppm by weight A.R. potassium chloride in double distilled water was made up and placed in a glass corrosion cell similar to the one already described. The solution was deoxygenated by bubbling with oxygen free nitrogen for fifteen minutes.

One of the samples was held potentiostatically for sixty minutes at a potential of - 0.85V (10 mV more noble than the pitting potential). The corrosion current was recorded on a Y/T recorder. A slight back-pressure of deoxygenated nitrogen was maintained in the corrosion cell apparatus to prevent atmospheric oxygen diffusing and dissolving in the test solution.

This procedure was repeated for each sample and the current/time traces recorded and labelled. An untreated sample of aluminium was also exposed to the chloride test solution at a potential of - 0.85V.

4.2.3 Results

The current produced with time when untreated aluminium is held potentiostatically at - 0.85V in double distilled water containing 100 ppm of potassium chloride is shown in Figure 19. The aluminium oxide film commences to breakdown after 4 minutes, and a pit has formed in 30 minutes. The pit may be seen on the surface after this time.

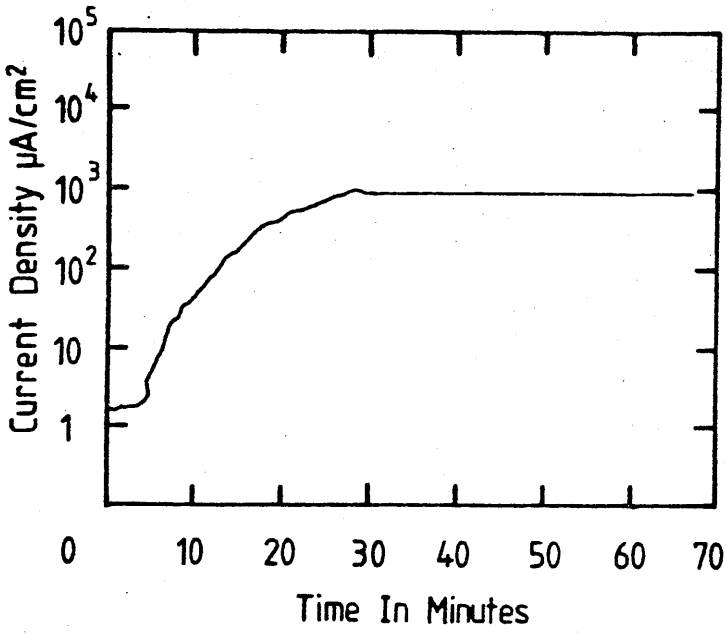

Figure 19 Current Time Relationship Of Untreated Aluminium In 100 ppm Potassium Chloride Solution At -0.85V

A typical current-time relationship for a treated aluminium sample with its fluoride film, in a solution containing 100 ppm of potassium chloride at a potential of - 0.85V is shown in Figure 20. Pit formation or aluminium oxide film breakdown does not start until about 25 minutes have elapsed and the development of a pit which may be seen with the naked eye takes about 60 minutes. It will be noted that the current is not constant even after this period of time.

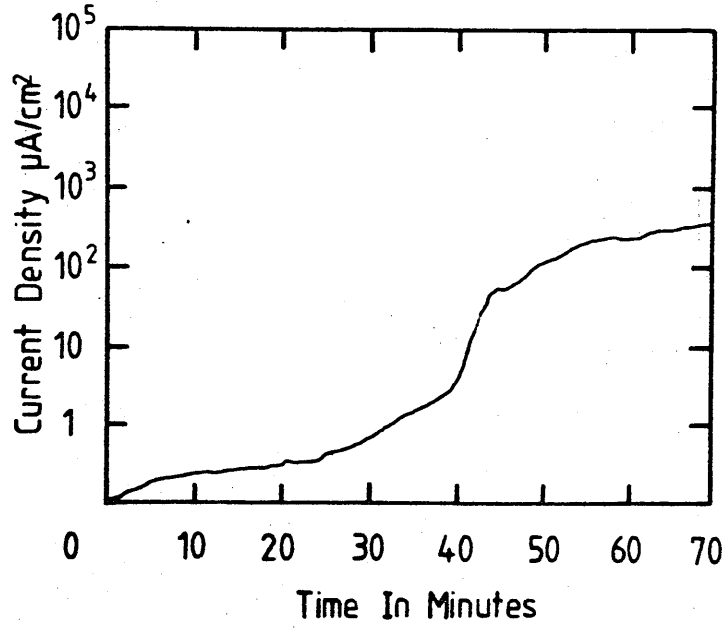

Figure 20 Current Time Relationship Of Aluminium With Thick Fluoride Film In 100 ppm Potassium Chloride Solution At -0.85V

The aluminium sample exposed to the solution of 50% ethanediol containing 100 ppm of sodium fluoride at a potential of - 0.85V, developed a tarnish film. The current time relationship of this treated aluminium sample when it was placed in a solution containing 100 ppm of potassium chloride at a potential of - 0.85V is shown in Figure 21.

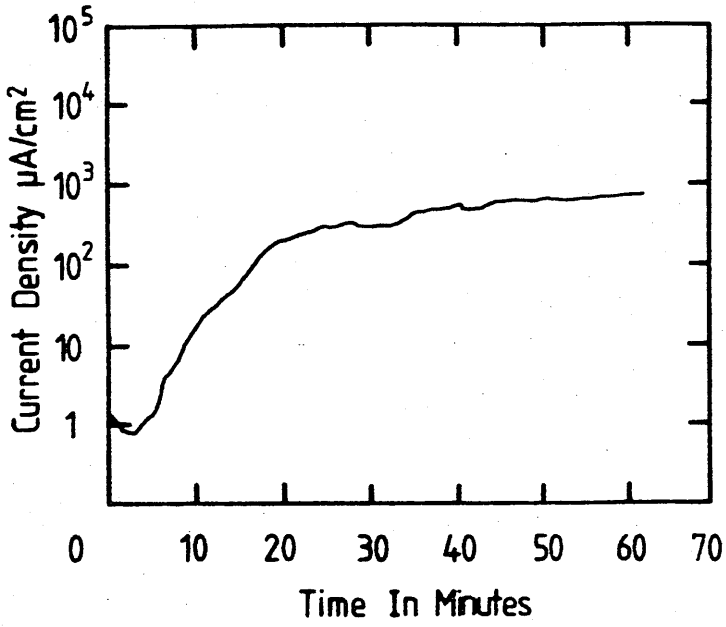

Figure 21 Current Time Relationship Of Aluminium With A Thin Fluoride Film In 100 ppm Potassium Chloride Solution At -0.85V

It will be observed that it is very similar to the curve obtained for an untreated specimen in chloride solution of double distilled water or 50% ethanediol at the same potential, Figure 19.

4.2.4 Conclusions

It is apparent that the fluoride film will not prevent pitting of aluminium samples placed in chloride solution at a potential of - 0.85V, but depending

on its thickness, it will delay the onset of pitting. However, in a fluoride solution at this potential, the film does prevent pitting and may even increase in thickness, depending on the potential, until - 0.59V is attained when film breakdown takes place and pits develop.

CHAPTER 5

5.0 Corrosion Cell Designed To Evaluate Effect Of Metal Ion Solution Concentration And Metal Ions Plating Out On The Corrosion Potential (Ecorr) Of Aluminium

The use of normal corrosion cells, as illustrated in Figure 15 for work involving heavy metals, e.g. lead or copper in solution, can lead to the following problems:-

(i) Some heavy metals plate out on the counter electrode, making any calculation of the amount of metal plating out onto the aluminium working electrode impossible.

(ii) The cost and time required to replace a 2 litre solution of varying concentration for each sample can be quite large.

(iii) There is also the risk of poisoning the reference electrode.

Therefore, to overcome these problems, it was necessary to design a corrosion cell which:-

(a) effectively isolated the reference electrode from the heavy metal cations, but allowed contact with the normal background solution ions. The working electrode would be exposed to the heavy metal ions as well as the normal ions.

(b) had two solutions separated by a permeable membrane.

(c) reduced the volume of heavy metal containing test solutions.

The problem was solved by constructing a cell within a cell. Diagrams and a description of the inner cell are given below, Figures 22 and 23, and its relationship to the outer corrosion cell is illustrated in Figure 24.

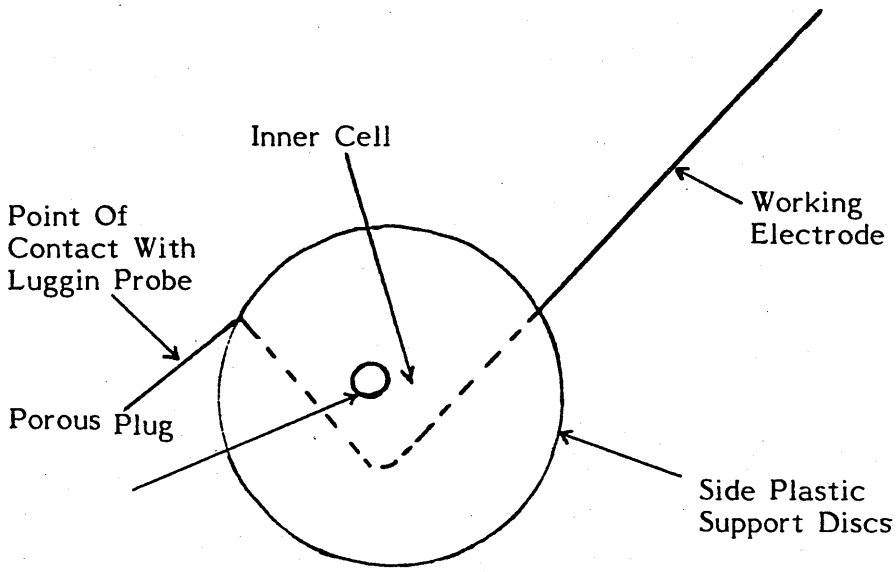

Figure 22 Diagram Of Side View Of Inner Aluminium Corrosion Cell

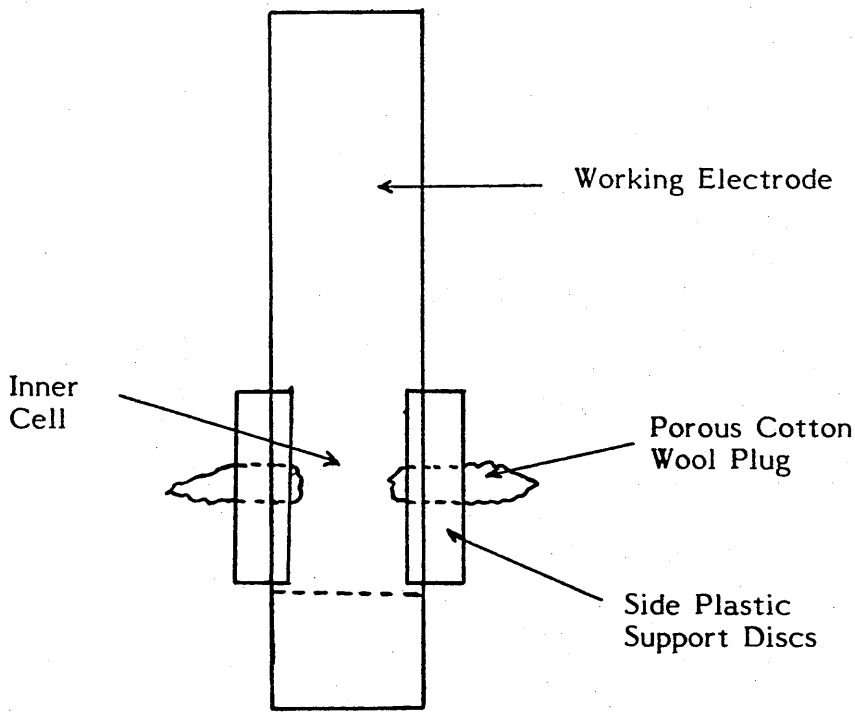

Figure 23 Diagram Of Front View Of Inner Aluminium Corrosion Cell

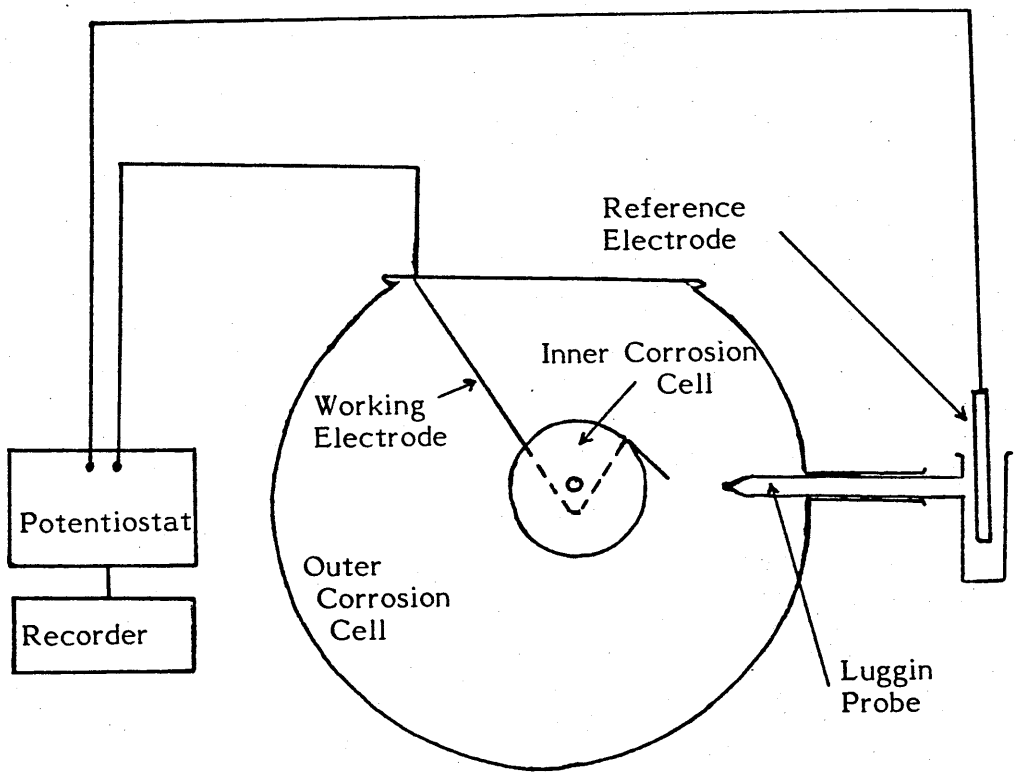

Figure 24 Schematic Diagram Of Inner And Outer Corrosion Cell Apparatus

The side plastic support discs were constructed by fusing an aluminium strip of similar thickness to the test material and 2 mm width into a disc of plastic, and after the plastic compound had solidified the aluminium was removed by dissolving it in hydrochloric acid, two of these discs were produced, one for the left side and the other for the right hand side of the cell.

Holes were drilled in the centre of each disc.

The aluminium test foil was then bent into a "Z" shape, and the edges of the test sample slotted into the plastic side disc, thus creating a V-shaped cell adjacent to the holes drilled in the plastic discs, with one very long arm (5 cm) connected to the working electrode of the potentiostat. The last leg of the "Z" shape (short leg), protruded over the edge of the cell and into the outer corrosion cell electrolyte. This part of the working electrode is in contact with the outer corrosion cell electrolyte and Luggin probe.

The holes in the plastic side discs were filled with porous cotton wool plugs to allow solution contact between the inner corrosion cell to outer corrosion cell.

It can be seen that the inner cell is a modified working electrode which fits into the normal corrosion cell system illustrated in Figure 24.

During corrosion trials, the outer cell (capacity 2000 mls) was filled with the background solution, having a similar halide concentration as the inner test cell solution when working on heavy metal cation effect.

The inner cell (capacity 3 mls) is filled with the test solution containing the desired concentration of heavy metal cations.

The Luggin probe was positioned at a convenient distance from the short arm of the "Z" shaped sample protruding into the outer cell to reduce the I.R. effect to a minimum.

The back surface of the aluminium working electrode was coated with petroleum jelly to insulate it from the electrolyte in the outer cell.

5.1 Investigation To Evaluate The Effect Of Lead Cations On The Corrosion Potential (Ecorr) Of Aluminium In Separate Solutions Of Fluoride, Chloride and Bromide Anions In Double Distilled Water And 50% Ethanediol Double Distilled Water

5.1.1 Equipment

Aluminium foil of 100 μm thickness and composition as given in section 2.2 was cut into strips 10 cm long x 1.5 cm wide. These strips were then degreased in acetone and dried. They were then inserted into the plastic side discs to a depth of 2 mm on each side leaving an exposed width of 11 mm. Figure 23. The potentiostatic equipment was as described in section 3.2.

The following six stock solutions were made up using A.R. 50% ethanediol and double distilled water.

(1) 200 ppm by weight A.R. potassium chloride.

(2) 200 ppm by weight A.R. potassium bromide.

(3) 200 ppm by weight A.R. sodium fluoride.

(4) 200 ppm by weight A.R. lead chloride.

(5) 200 ppm by weight A.R. lead bromide.

(6) 200 ppm by weight A.R. lead fluoride.

The molecular weights of the main elements used in this trial are listed below.

Element	Molecular Weight g/mol
Lead	207.20
Chlorine	35.45
Bromine	79.90
Fluorine	18.99
Sodium	22.98
Potassium	39.10

Due to difference in molecular weights, a 200 ppm by weight solution of potassium chloride does not contain the same amount of chloride or number of chloride anions as lead chloride. In order that any corrosion potential shift is due to the presence of lead cations, the actual concentration of halide anions in the inner and outer corrosion cell solution must be the same. This can be achieved by adding a calculated volume of alkaline halide of known concentration solution to the lead halide test solution. The list below gives the normal formulae of the various reagents used along with their molecular weight and amount of halide in 0.1g.

Normal Formula	Molecular Weight	Weight Of Halide In 0.1g Reagent
Lead Chloride ($PbCl_2$)	278.00 g	0.025 g
Lead Bromide ($PbBr_2$)	367.00 g	0.043 g
Lead Fluoride (PbF_2)	245.18 g	0.015 g
Sodium Fluoride (NaF)	41.97 g	0.045 g
Potassium Chloride (KCl)	74.55 g	0.047 g
Potassium Bromide (KBr)	119.00 g	0.067 g

For the corrosion trial, five concentrations 10, 20, 40, 80 and 100 ppm by weight of each lead halide salt, in both double distilled water and 50% ethanediol double distilled water, were required.

100 mls of each of the test solutions of various lead halide salt concentration were made up and the halide level was balanced by the addition of extra alkaline halide solution. Table 18 lists the weight of halide in the concentration of lead halide salt selected, gives the target weight of halide and the shortfall. These are then used to determine the volume of lead halide and alkaline metal halide solution required to produce the solution with the desired anion and cation concentration.

The table applies equally to the 50% ethanediol solution, the only difference being that a 50% ethanediol double distilled water solution is used to dilute the solution to 100 mls.

5.1.2 Method

The outer cell was first filled (2 litres) with a 100 ppm by weight solution of the respective alkaline metal halide salts, e.g. sodium fluoride for lead fluoride test solution. When the inner cell solution was made up using lead halide distilled water, then the outer cell was filled with alkaline metal halide distilled water, but if lead halide 50% ethanediol were used in the inner cell, then alkaline metal halide 50% ethanediol distilled water solution was also used in the outer cell.

A degreased strip of aluminium was then slotted into the inner corrosion cell, and the back coated with petroleum jelly. Cotton wool plugs were then inserted into the side plates. The inner cell was then connected

to the potentio-galvano scan and lowered into the outer cell electrolyte, until the front plate of the inner cell was the prescribed distance away from the Luggin probe. The inner corrosion cell was then filled with 3 mls of the outer electrolyte as a control experiment and the corrosion potential was recorded for twenty minutes.

The inner corrosion cell test aluminium foil was changed after the initial control experiment, and the inner cell replaced in the outer cell and then filled with 3 mls of the lowest concentration lead halide solution and the corrosion potential against time recorded for twenty minutes. This procedure was repeated for each of the lead halide concentrations. The background electrolyte was then discarded and fresh background solution placed in the outer cell of a different alkaline metal halide salt solution, or a halide salt in 50% ethanediol double distilled water.

The control experiment was carried out with each new outer electrolyte with the lead halide test solutions. These procedures were repeated until all outer electrolytes, and hence all the lead halide solutions, had been tested.

5.1.3 Results

Typical potential time trace for 100 ppm lead fluoride solution is shown in Figure 25. The solution was added after 30 seconds and the corrosion potential attained was - 1.10V. There was no pitting of the aluminium, since the corrosion potential was more negative than the critical pitting potential of - 0.59V. The results are summarised in Table 19.

Potential/time curves for the chloride solution are given in Figure 26 for 10 ppm lead chloride and Figure 27 for 20 ppm lead chloride.

Pitting develops in the 20 ppm lead chloride solution and in the more concentrated lead chloride solutions, but not in the 10 ppm solution. The relationship of the corrosion potentials to the pitting potentials is shown in Figures 26 and 27, and the results are summarised in Table 19. It will be observed from Figure 26 that the corrosion potential is more negative than the pitting potential and in Figure 27, the corrosion potential oscillates around the value of the pitting potential.

There was no pitting observed in the bromide containing solution, Figure 28 and Table 19.

5.2 Investigation To Evaluate The Effect Of Copper Cations On The Corrosion Potential Of Aluminium In 100 ppm By Weight Solution Of Potassium Chloride In Both Double Distilled Water And 50% Ethanediol Double Distilled Water

The previous experiment was repeated using five concentrations by weight of copper II chloride in double distilled water and 50% ethanediol double distilled water, namely 1, 2, 5, 10 and 20 ppm.

In order to be certain that any corrosion potential shifts are due to the presence of copper cations, the actual concentration of chloride ions in the inner and outer cell solutions must be the same. This can be achieved by adding a calculated volume of potassium chloride of known concentration to the copper chloride test solutions as previously described.

5.2.1 Results

A potential time curve for 1 ppm copper chloride solution is shown in Figure 29.

The solution was added after 30 seconds and the corrosion potential attained was - 0.95V. There was no pitting of the aluminium, since the corrosion potential was more negative than the critical pitting potential of - 0.91V.

In the 2 ppm solution, Figure 30, and more concentrated solutions, pitting develops. The results are summarised in Table 21.

5.2.2 Conclusions

The degree of corrosion potential shift of aluminium in the noble direction increased with increase in lead concentration for lead fluoride, bromide and iodide. The corrosion potential did not reach the Ep value for lead halide concentrations in the range 0 - 100 ppm by weight for these three lead halide salt solutions, although it is possible that Ep could be attained if the lead concentration were increased sufficiently.

In the case of lead chloride, the Ep value was exceeded at a lead chloride concentration of 20 ppm. The nobility then decreased to the Ep value and oscillated around this potential, Figure 27, pitting corrosion then taking place. The potential traces for lead chloride concentration of 20 ppm and above, with 100 ppm of chloride anion by weight were similar to Figure 27, with pitting corrosion taking place in each case.

The corrosion potential of aluminium reached the Ep value, when it was exposed to a copper chloride concentration of 2 ppm, Figure 30, and above, the trace being similar to that for 20 ppm lead chloride with corrosion potential oscillating around the Ep value. This much lower concentration of copper cations required to shift the aluminium corrosion potential into the pitting corrosion range compared with that for lead cations, would be expected from their relative positions in the electrochemical series, copper being far more noble than lead.

5.3 Investigation To Determine The Relationship Of Corrosion Potential Shift Of The Aluminium Inner Corrosion Cell With Change In Lead Cation Concentration Against Time

5.3.1 Equipment

The potentiostatic equipment was the same as described in section 3.2.

5.3.2 Method

A single concentration for each of the three lead halide salts (lead fluoride, lead chloride and lead bromide) was selected in both double distilled and 50% ethanediol solutions for the inner corrosion test cell. These test solutions were made up using the 200 ppm stock solutions used in the initial potential shift/lead halide concentration investigations, care was taken to maintain the balance of halide concentration in the inner and outer corrosion cell.

The lead concentration in each test solution was determined using an atomic absorption spectrophotometer. A degreased strip of aluminium was then slotted into the inner corrosion cell, and the back coated with petroleum jelly. Cotton wool plugs were then inserted into the side plates. The inner cell was then placed in the working electrode clamp of the potentio-galvano scan and lowered into the outer cell electrolyte until the front plate of the inner cell was the prescribed distance away from the Luggin probe to reduce I.R. effects.

In order to evaluate the rate of lead halide change against time, five exposure times of the aluminium were selected, 30, 60, 180, 360 and 600 seconds.

The corrosion cell was filled with a three centimetre cubed sample of the lead halide test solution under investigation. After the first exposure period of 30 seconds, two centimetre cubed of the inner corrosion cell test solution was removed. The inner cell was then dismantled and a fresh aluminium sample slotted in, the inner cell was then refilled with fresh solution and exposed for the second time interval and a sample was taken for lead analysis. This procedure was repeated until the five exposure periods were covered for each of the lead halide salts in double distilled water and 50% ethanediol. The lead content of the test solutions after various exposure times are given in Table 22.

5.3.3 Results

The variation in potential for lead fluoride, chloride and bromide is shown in Figures 31, 32 and 33 and the change in lead concentration of solution with time is superimposed on each diagram.

5.4 Investigation To Determine The Relationship Of Corrosion Potential Shift Of The Aluminium Inner Corrosion Cell With Change In Copper Cation Concentration Against Time

The previous experiment was repeated using copper II chloride in double distilled water and 50% ethanediol solution, and the results are given in Table 23 and Figure 34.

5.5. Conclusions

It can be seen from Figures 31, 32 and 33, that for approximately 60 - 70 seconds after the addition of the lead cation containing solution, there is no decrease in the lead concentration although there is a rapid movement of the corrosion potential in the noble direction. A similar induction period was also observed for copper II chloride in double distilled water and 50% ethanediol.

The investigation of lead deposit distribution on aluminium samples exposed to lead chloride double distilled water solution for various lengths of time, using a scanning electron microscope microprobe, also concluded that no lead was deposited on the aluminium surface in the first 60 seconds of exposure.

The halide anion concentration of the inner and outer cell electrolytes is constant for all cases and since ion selective electrode measurements show that the activities of the electrolytes are similar, the shift in corrosion potential must be related to the lead cations in the electrolyte.

The movement of the corrosion potential in the noble direction of aluminium exposed to a solution containing heavy metal cations e.g. lead or copper,

has always been considered to be caused by the formation of galvanic cells on the surface of the exposed aluminium by deposition of the more noble metal. Since the corrosion potential shift in the present investigation takes place before the deposition, this cannot be the case. The corrosion potential shift must be associated with lead and copper cations in solution rather than the deposits of these metals.

It is well known that metals, when exposed to electrolytes, develop electrical double layer, or Helmholtz plane, Figure 40.
The inner Helmholtz plane being a negative layer of electrons on the metal surface, the outer layer being positively charged cations of the base metal sheathed and separated from the metal surface by water molecules. The metal cation layer gradually phases out as the distance from the metal surface increases and merges with the bulk electrolyte of normal properties. This dispersed area is called the Gouy-Chapman layer.

It is proposed that the movement of the corrosion potential of aluminium exposed to lead and copper cation containing solutions is caused by the migration of the lead or copper cations which are of different ionic radii, charge number and, more importantly, greater electron affinity than the aluminium cation into the aluminium cation rich outer Helmholtz plane, disrupting the charge distribution and hence the distribution of the surface electrons (inner Helmholtz plane). Figure 41.

The surface electrons would probably migrate on the aluminium surface to align themselves with the stronger charge field of the heavy metal

cations, thus causing localized concentrations of electrons and hence creating sites of lower electron density and weaker negative charge elsewhere on the aluminium surface. These electron deficient sites would allow halide anions to penetrate the passive alumina film more freely.

The change in electron distribution and resultant corrosion potential shift would also stimulate the formation of Al^{3+} cations and the resultant release of electrons at the sites of electron deficiency, reaction

$$Al \rightarrow Al^{3+} + 3e^{-}$$

Pryor proposed that halide anions incorporated in the alumina film increases the aluminium cation diffusion rate through the film. Therefore, when halide anions enter the alumina film at the electron deficient sites, the aluminium cations which formed in an attempt to restore the electron density at these points would diffuse through the alumina film, initiating pitting.

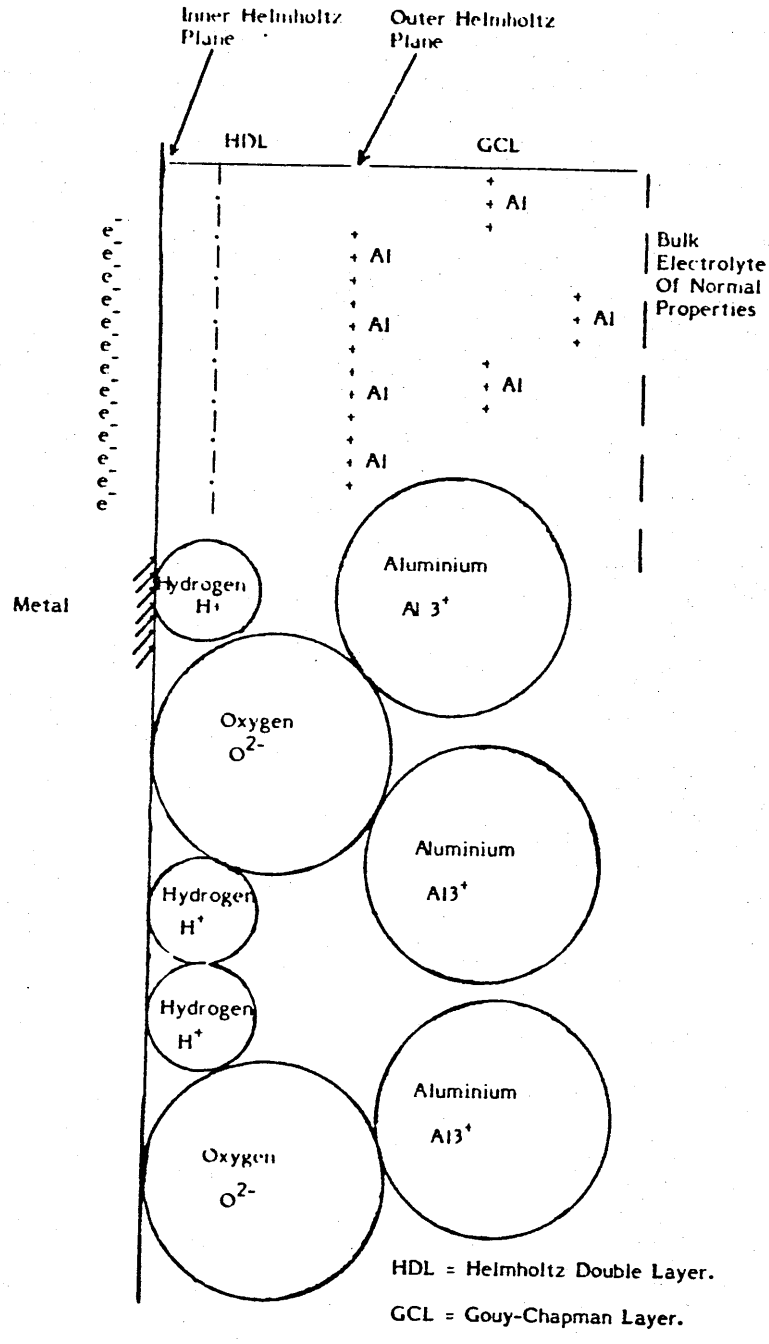

Figure 40 Schematic Diagram Of Aluminium's Double Electric Layer Which Forms On Exposure To Electrolyte Free From Cations

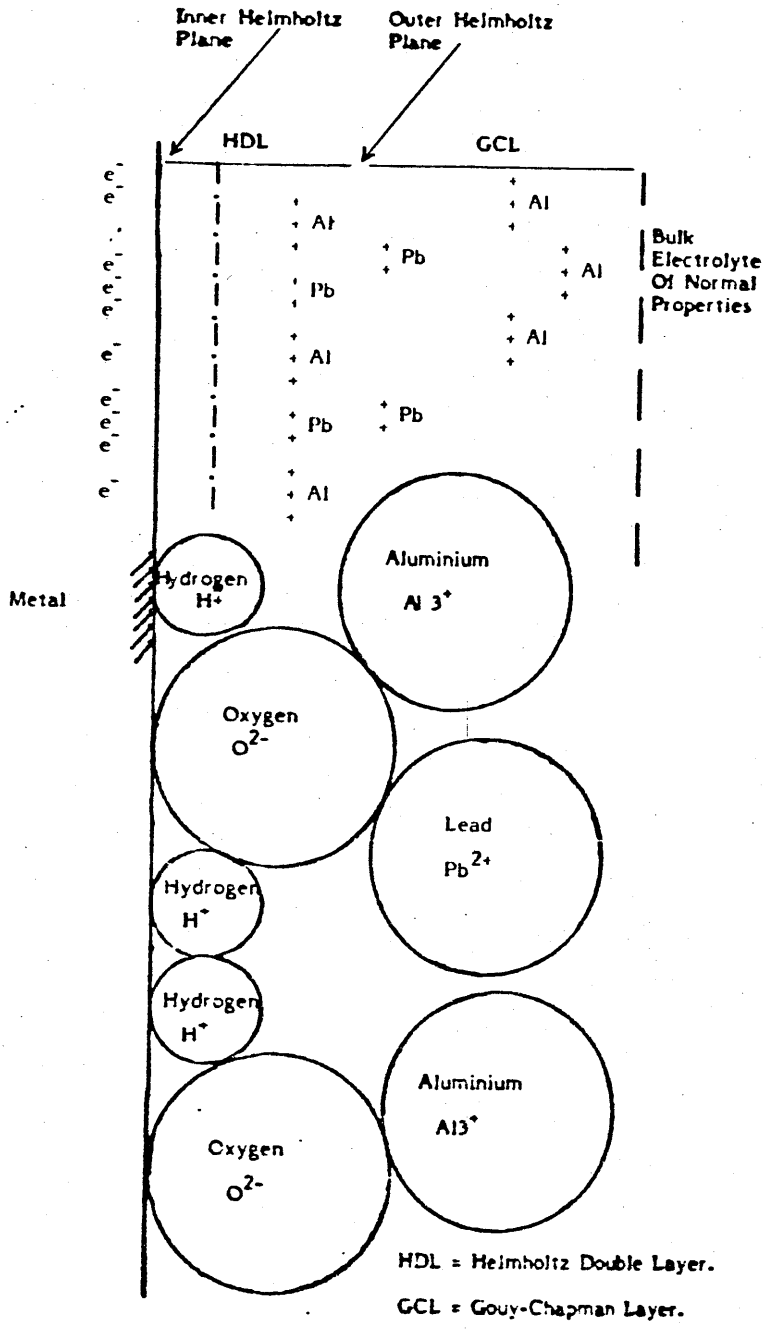

Figure 41 Schematic Diagram Of Aluminium's Double Electric Layer Which Forms On Exposure To Electrolyte Containing Lead Cations

Table 18

Compositions Of The Inner Corrosion Cell, Lead Halide Test Solutions

Halide Salt	Concentration By Weight	Weight Halide	Target Halide Weight	Shortfall	Volume 200 ppm Lead Halide Solution	Volume 200 ppm Alkaline Metal Halide Solution	Volume Of Double Distilled Water
Lead Chloride	10 ppm	0.0025 g	0.047 g	0.0445 g	5 mls	47.3 mls	47.7 mls
	20 ppm	0.0050 g	0.047 g	0.0420 g	10 mls	44.7 mls	45.3 mls
	40 ppm	0.0100 g	0.047 g	0.0370 g	20 mls	39.3 mls	40.7 mls
	80 ppm	0.0200 g	0.047 g	0.0270 g	40 mls	28.7 mls	31.3 mls
	100 ppm	0.0250 g	0.047 g	0.0220 g	50 mls	23.4 mls	26.6 mls
Lead Bromide	10 ppm	0.0043 g	0.067 g	0.0627 g	5 mls	46.8 mls	48.2 mls
	20 ppm	0.0086 g	0.067 g	0.0584 g	10 mls	43.6 mls	46.4 mls
	40 ppm	0.0172 g	0.067 g	0.0498 g	20 mls	37.2 mls	42.8 mls
	80 ppm	0.0344 g	0.067 g	0.0326 g	40 mls	24.3 mls	35.7 mls
	100 ppm	0.0430 g	0.067 g	0.0240 g	50 mls	18.0 mls	32.0 mls
Lead Fluoride	10 ppm	0.0015 g	0.045 g	0.0435 g	5 mls	48.3 mls	46.7 mls
	20 ppm	0.0030 g	0.045 g	0.0420 g	10 mls	46.6 mls	43.4 mls
	40 ppm	0.0060 g	0.045 g	0.0390 g	20 mls	43.3 mls	36.7 mls
	80 ppm	0.0120 g	0.045 g	0.0330 g	40 mls	36.6 mls	23.4 mls
	100 ppm	0.0150 g	0.045 g	0.0300 g	50 mls	33.3 mls	16.7 mls

Table 19

Effect Of Lead Concentration On The Corrosion Potential Of Aluminium

Total Halide Conc. (In ppm)	Lead Halide Conc. (In ppm)	Distilled Water (Corrosion Potential)		50% Ethanediol (Corrosion Potential)	
Fluoride	0	- 1.29V	No Pitting	- 1.25V	No Pitting
100 ppm	10	- 1.29V	No Pitting	- 1.22V	No Pitting
	20	- 1.18V	No Pitting	- 1.17V	No Pitting
	40	- 1.14V	No Pitting	- 1.18V	No Pitting
	80	- 1.12V	No Pitting	- 1.15V	No Pitting
	100	- 1.10V	No Pitting	- 1.08V	No Pitting
Chloride	0	- 0.98V	No Pitting	- 0.97V	No Pitting
100 ppm	10	- 0.98V	No Pitting	- 1.00V	No Pitting
	20	- 0.90V	Pitting	- 0.97V	No Pitting
	40	- 0.91V	Pitting	- 0.91V	Pitting
	80	- 0.90V	Pitting	- 0.95V	Pitting
	100	- 0.89V	Pitting	- 0.89V	Pitting
Bromide	0	- 1.06V	No Pitting	- 0.98V	No Pitting
100 ppm	10	- 0.97V	No Pitting	- 1.23V	No Pitting
	20	- 0.92V	No Pitting	- 1.22V	No Pitting
	40	- 0.90V	No Pitting	- 1.16V	No Pitting
	80	- 0.87V	No Pitting	- 1.17V	No Pitting
	100	- 0.87V	No Pitting	- 1.04V	No Pitting

Mercury/Mercurous Sulphate Reference Electrode.

Table 20

Pitting Potential For 100 ppm By Weight Solution For Fluoride, Chloride and Bromide

Halide	Double Distilled Water	50% Ethanediol
Fluoride	- 0.59V	- 0.55V
Chloride	- 0.91V	- 0.89V
Bromide	- 0.77V	- 0.74V

Table 21

Effect Of Copper Concentration On The Corrosion Potential Of Aluminium

Copper Chloride Concentration In ppm By Weight	Double Distilled Water		50% Ethanediol Double Distilled Water	
1	- 0.95V	No Pitting	- 0.96V	No Pitting
2	- 0.86V	Pitting	- 0.90V	Pitting
5	- 0.86V	Pitting	- 0.87V	Pitting
10	- 0.85V	Pitting	- 0.87V	Pitting
20	- 0.85V	Pitting	- 0.86V	Pitting

Table 22

Table Of Analysis Results Of Lead Halide Solutions, Double Distilled And 50% Ethanediol, Exposed To Aluminium In A Corrosion Cell For Various Lengths Of Time

Halide Salt	Time Exposed	Double Distilled Water (Lead in ppm)	50% Ethanediol (Lead in ppm)
Lead Chloride 100 ppm by Weight	Initial	74.0 ppm	74.0 ppm
	30 sec.	74.0 ppm	74.0 ppm
	1 min.	74.0 ppm	74.0 ppm
	3 min.	71.6 ppm	62.9 ppm
	6 min.	69.8 ppm	61.4 ppm
	10 min.	68.2 ppm	60.0 ppm
Lead Bromide 100 ppm by Weight	Initial	56.0 ppm	55.0 ppm
	30 sec.	56.0 ppm	55.0 ppm
	1 min.	56.0 ppm	55.0 ppm
	3 min.	54.1 ppm	55.0 ppm
	6 min.	54.1 ppm	53.1 ppm
	10 min.	53.0 ppm	51.4 ppm
Lead Fluoride 100 ppm by Weight	Initial	83.0 ppm	82.6 ppm
	30 sec.	83.0 ppm	82.6 ppm
	1 min.	83.0 ppm	82.6 ppm
	3 min.	80.5 ppm	81.7 ppm
	6 min.	77.3 ppm	81.0 ppm
	10 min.	75.0 ppm	79.0 ppm

Table 23

Table Of Analysis Results Of Copper II Chloride Solutions In Double Distilled Water And 50% Ethanediol, Exposed To Aluminium In A Corrosion Cell For Various Lengths Of Time

Time In Seconds	Double Distilled Water (Copper in ppm)	50% Ethanediol (Copper in ppm)
Initial	97.50	97.50
30	97.50	97.50
60	97.50	97.50
120	96.20	97.50
180	92.50	97.50
360	90.70	96.66
600	82.00	95.72

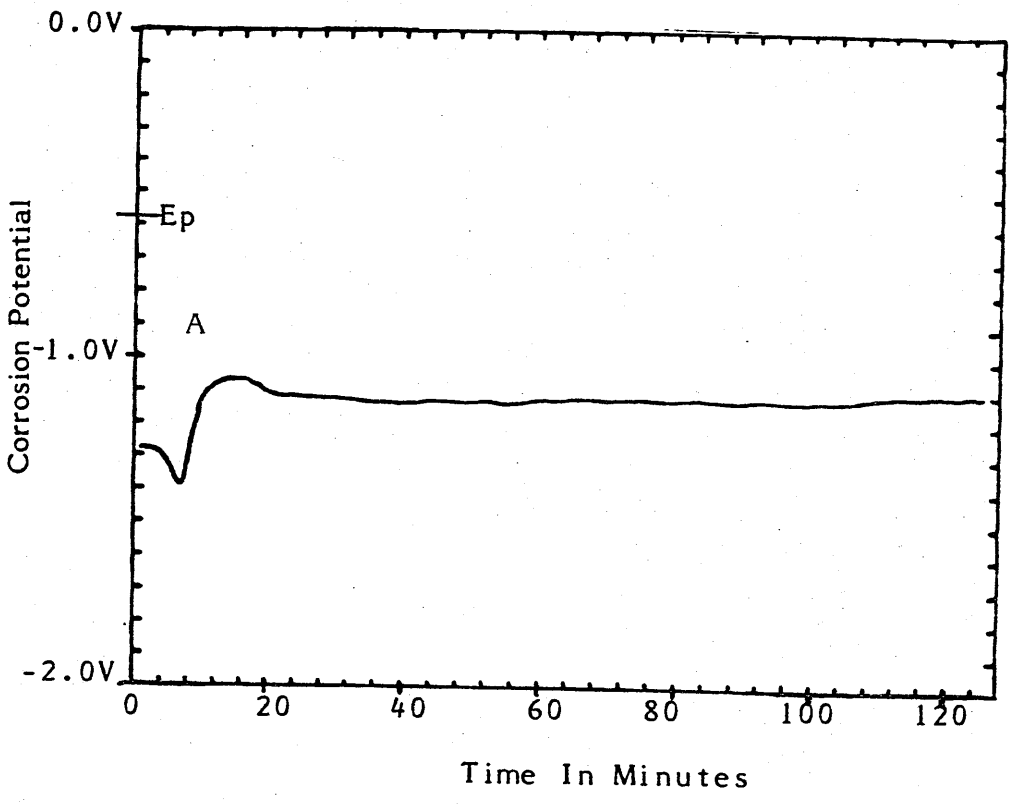

Figure 30 Graph of corrosion potential against time for an aluminium corrosion cell filled with 3 mls of 100 ppm by weight lead fluoride solution with an addition of sodium fluoride to maintain the halide balance.

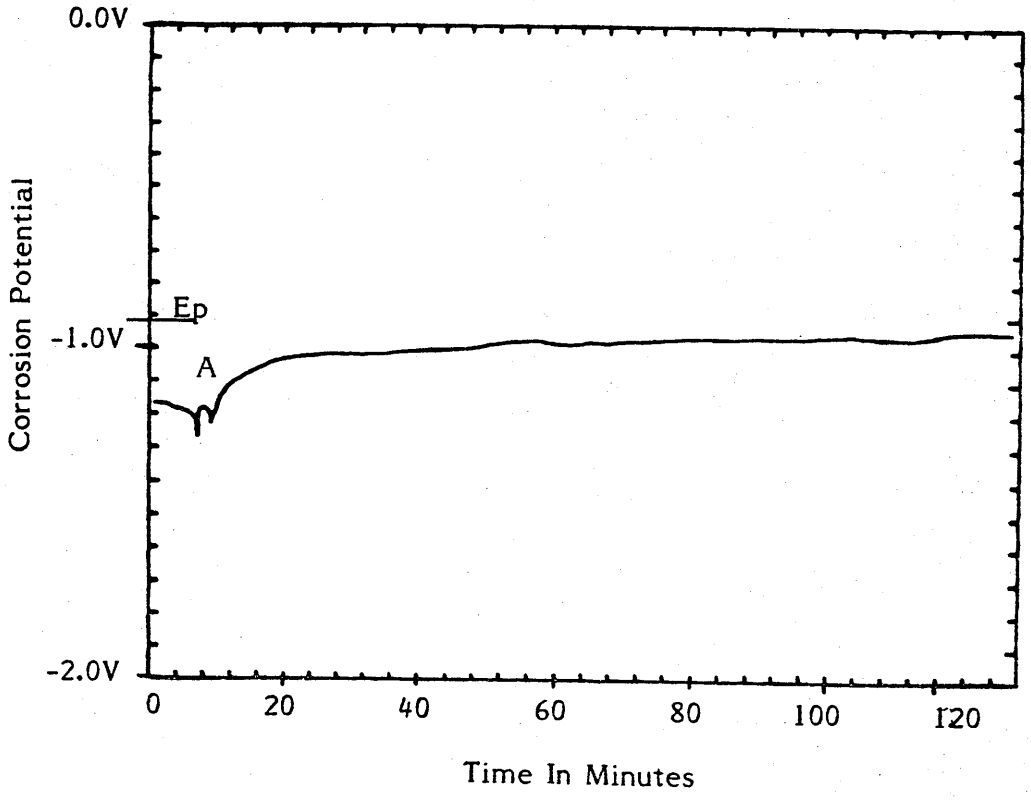

Figure 31 Graph of corrosion potential against time for an aluminium corrosion cell filled with 3 mls of 10 ppm by weight lead chloride solution with an addition of potassium chloride to maintain the halide balance.

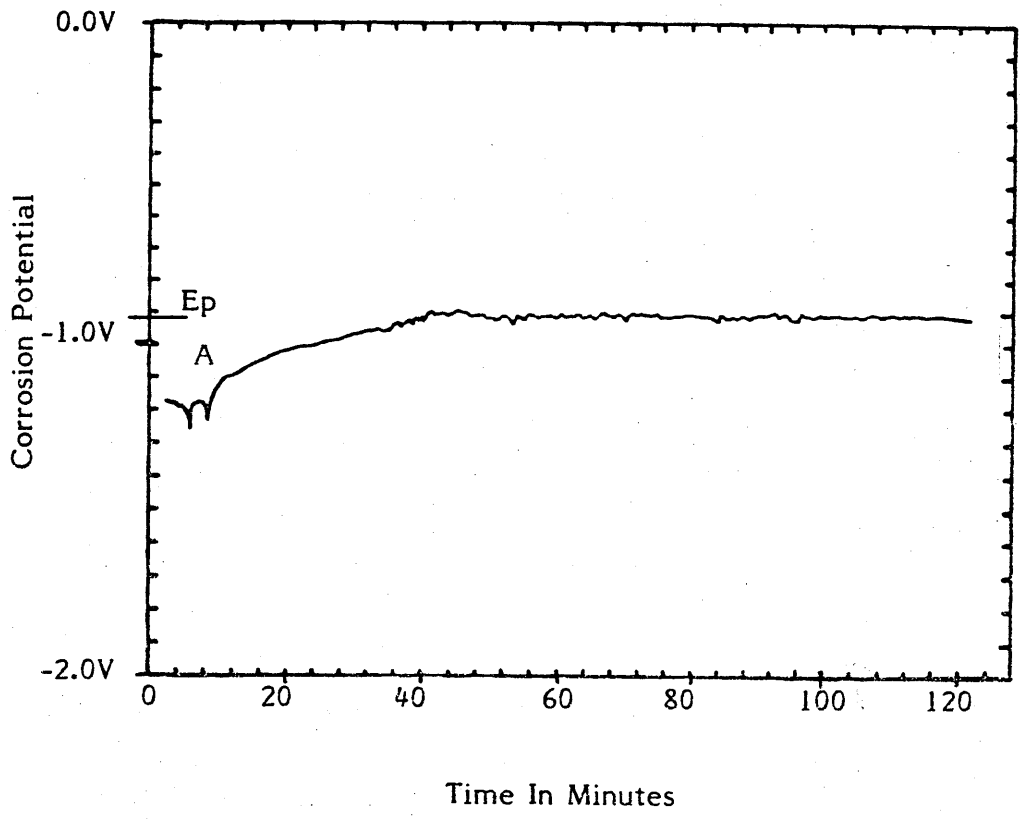

Figure 32 Graph of corrosion potential against time for an aluminium corrosion cell filled with 3 mls of 20 ppm by weight lead chloride with an addition of potassium chloride to maintain the halide balance.

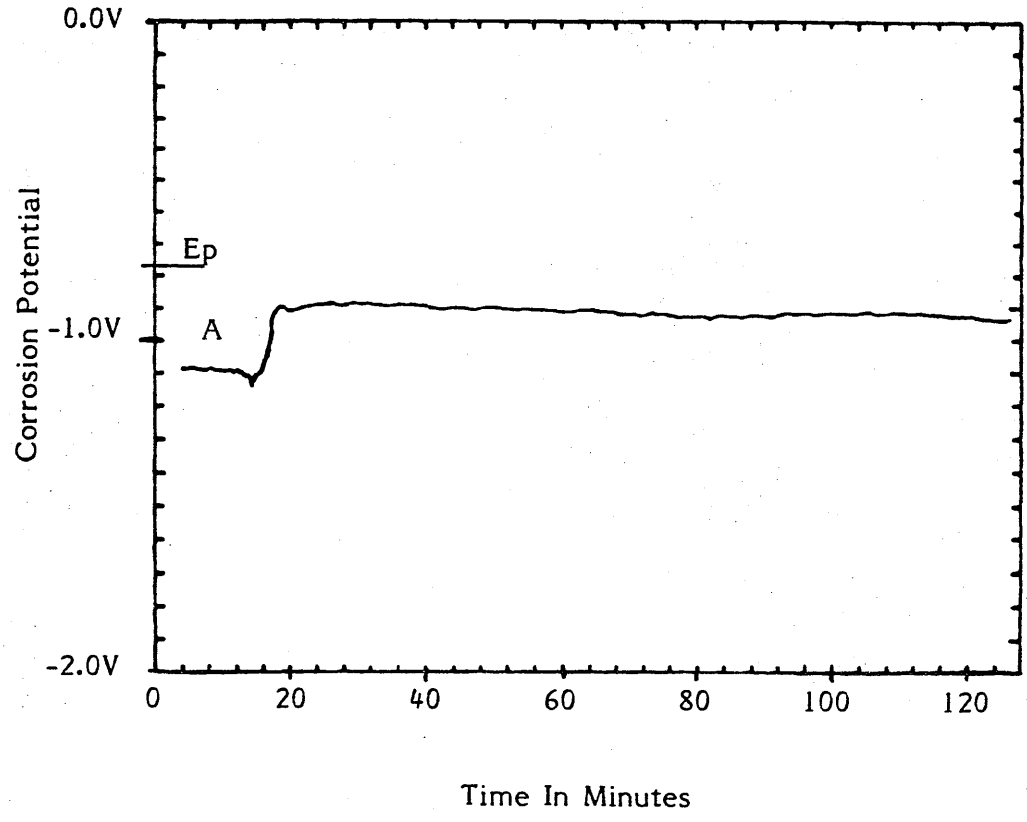

Figure 33 Graph of corrosion potential against time for an aluminium corrosion cell filled with 3 mls of 100 ppm by weight lead bromide solution with an addition of potassium bromide to maintain the halide balance.

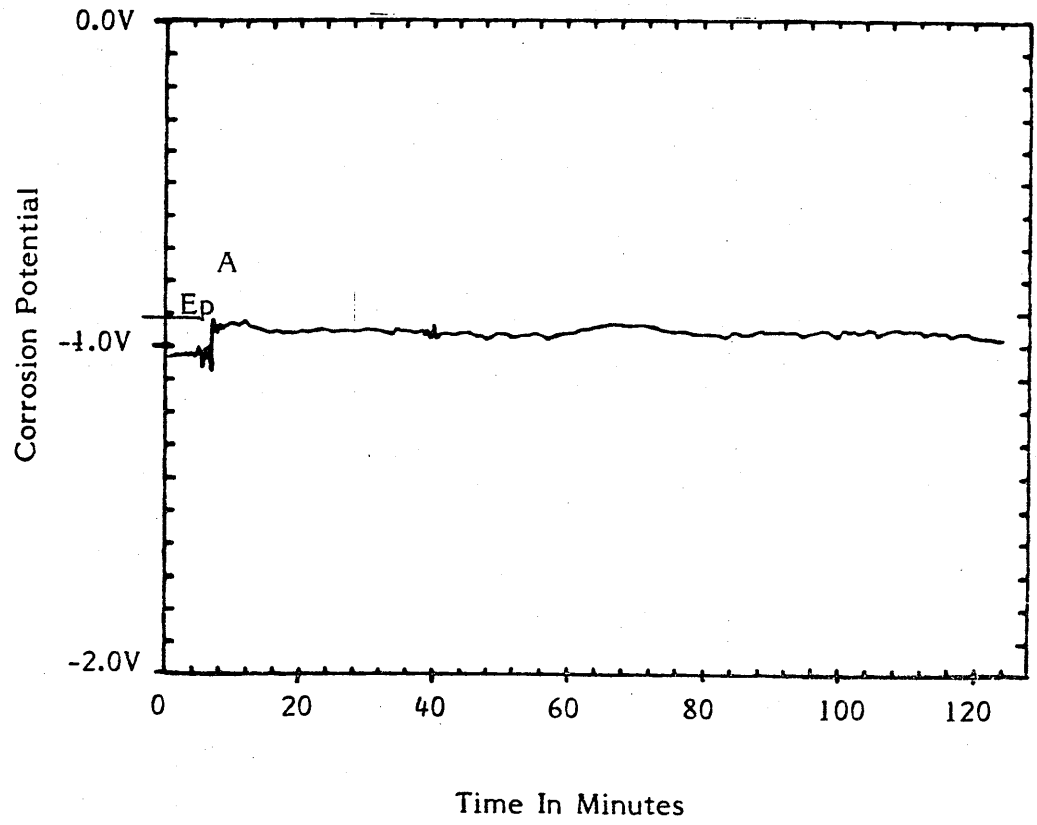

Figure 34 Graph of corrosion potential against time for an aluminium corrosion cell filled with 3 mls of 1 ppm by weight copper II chloride with an addition of potassium chloride to maintain the halide balance.

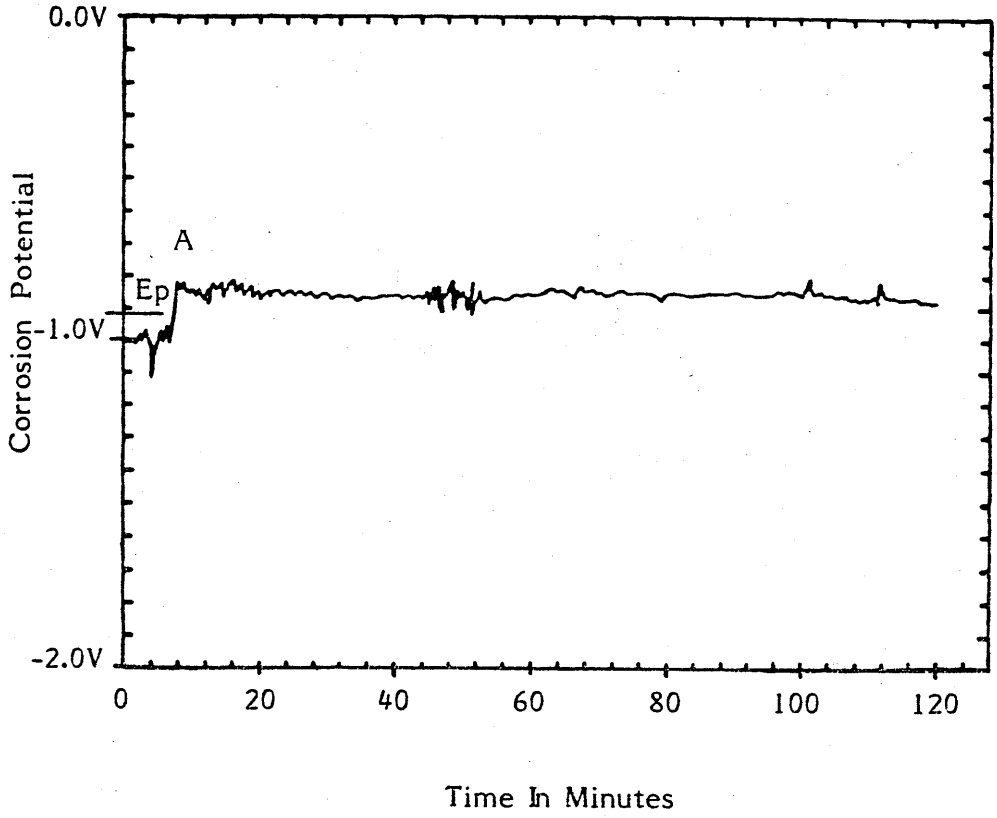

Figure 35 Graph of corrosion potential against time for an aluminium corrosion cell filled with 3 mls of 2 ppm by weight copper II chloride solution with an addition of potassium chloride to maintain halide balance.

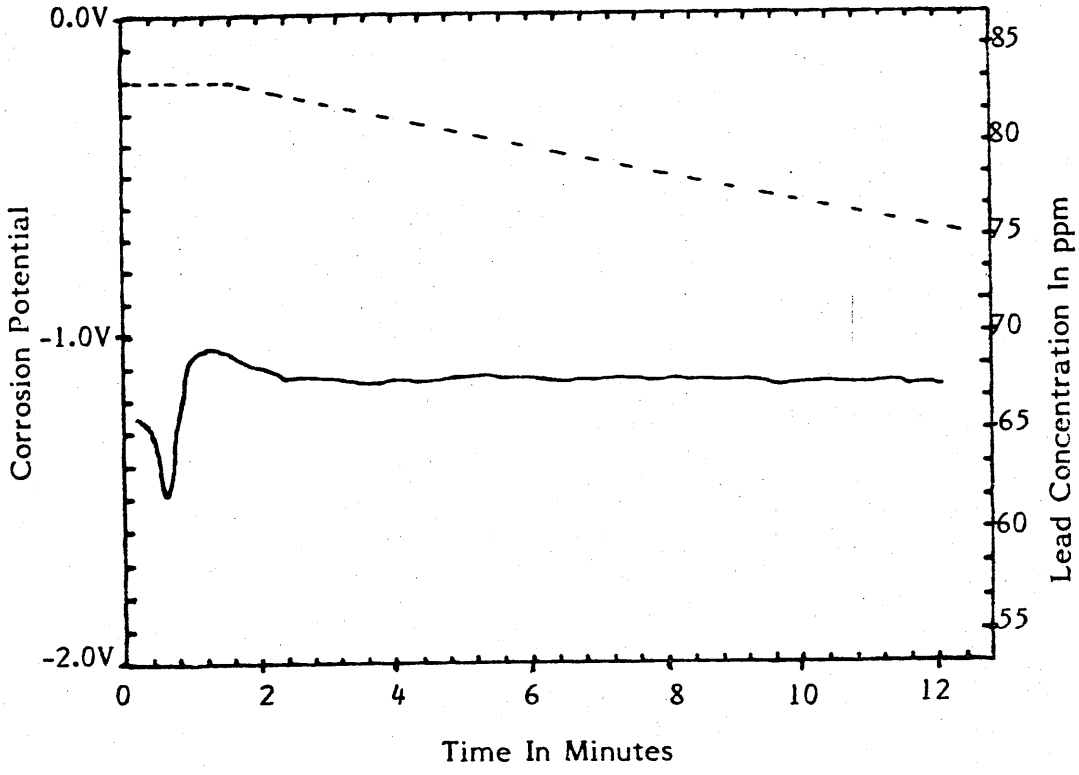

Figure 36 Graph of lead concentration and corrosion potential of an aluminium corrosion cell (filled with 3 mls of lead fluoride solution) against time.

_____ Corrosion Potential

---------- Lead Concentration

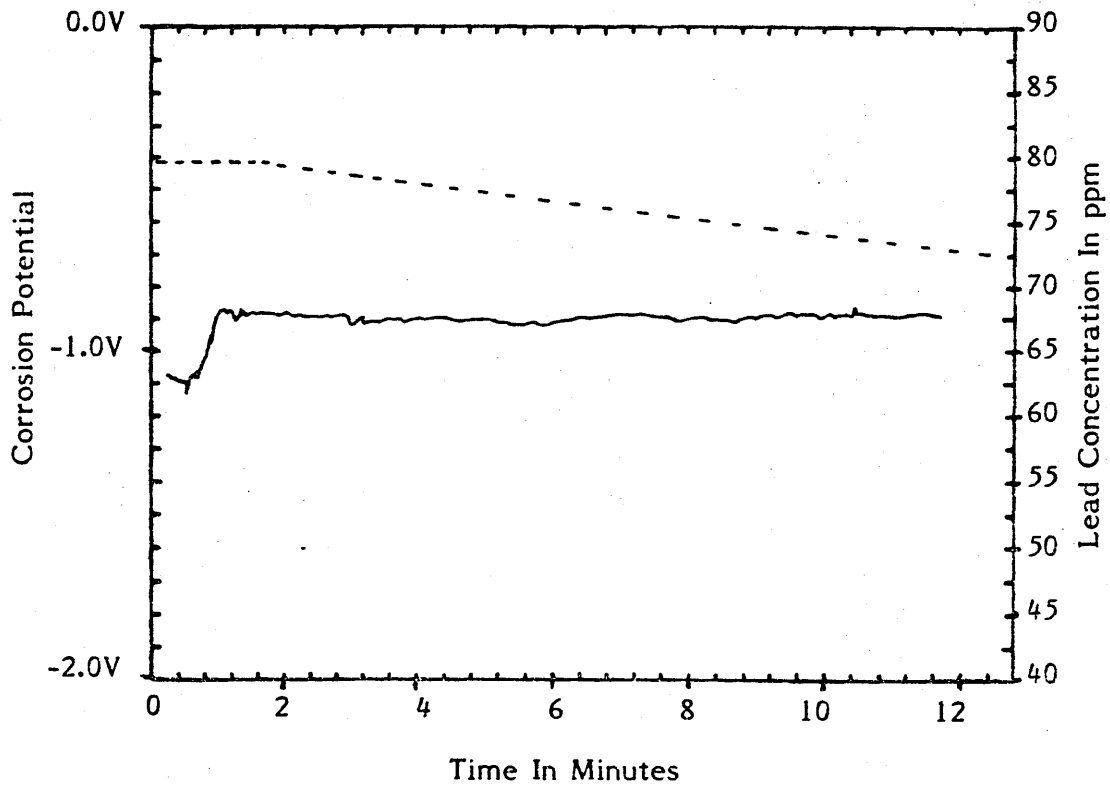

Figure 37 Graph of lead concentration and corrosion potential of an aluminium corrosion cell (filled with 3 mls of lead chloride solution) against time.

_____ Corrosion Potential

---------- Lead Concentration

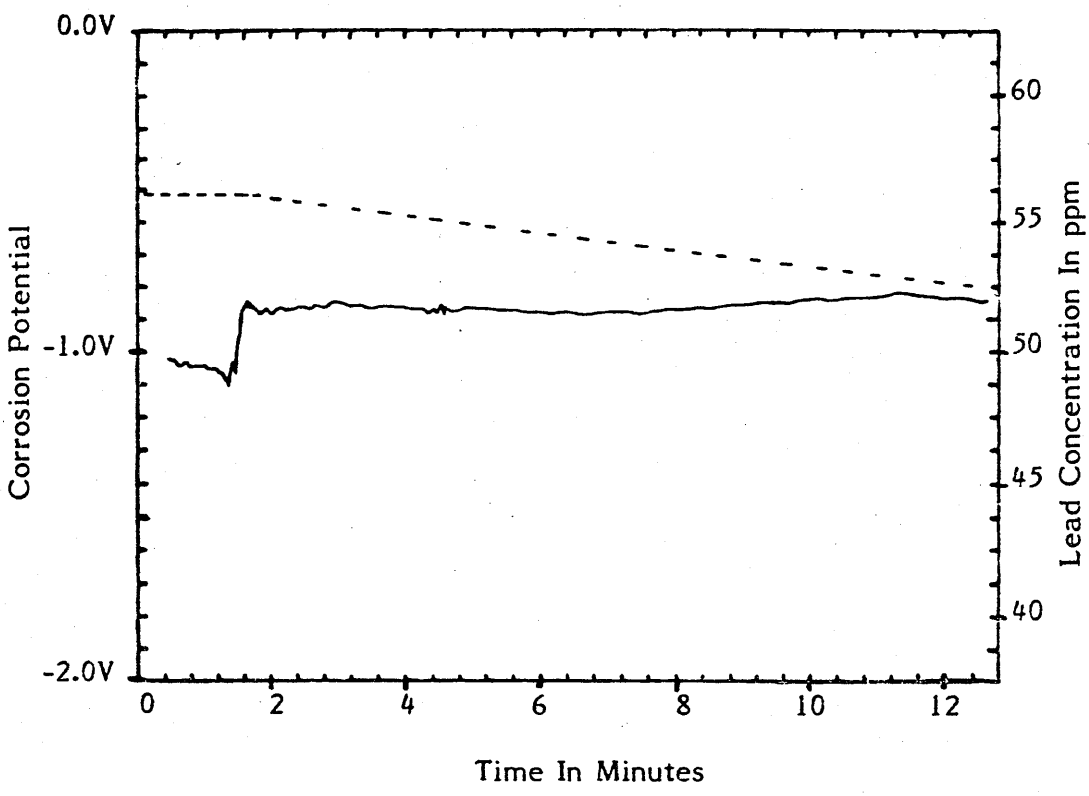

Figure 38 Graph of lead concentration and corrosion potential of an aluminium corrosion cell (filled with 3 mls of lead bromide) against time.

_____ Corrosion Potential

---------- Lead Concentration

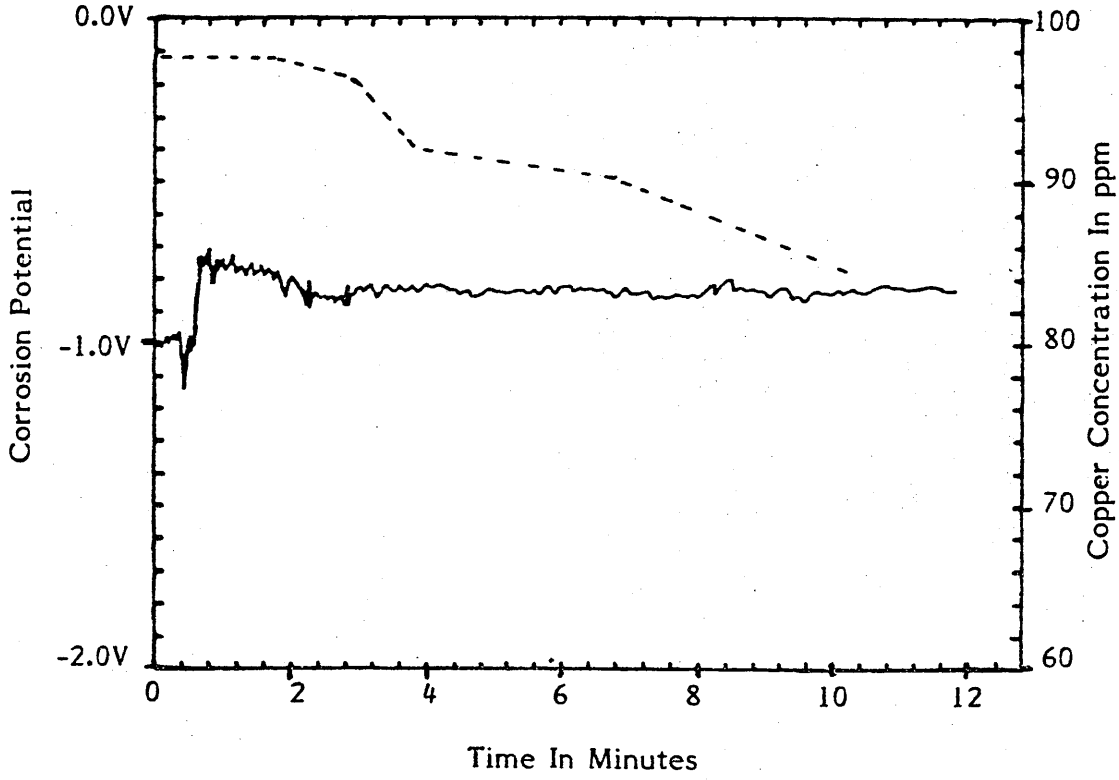

Figure 39 Graph of copper concentration and corrosion potential of an aluminium corrosion cell (filled with 3 mls of copper II chloride solution) against time.

_____ Corrosion Potential

---------- Copper Concentration

CHAPTER 6

6.0 General Conclusions And Discussions

The full conclusions are included in the relevant chapters and are only briefly reviewed below.

Of the range of metals and alloys used to construct the automobile engine and its cooling system, only aluminium, mild steel and low tin solders corrode at a high rate. The aluminium corrodes locally whilst the mild steel and low tin solders corroded uniformly.

The cations Pb^{2+}, Sn^{2+}, Fe^{2+} and Al^{3+} are released into the coolant as corrosion reaction products and the Fe^{2+} cations will be rapidly oxidised to the insoluble Fe^{3+} form, being precipitated out of solution. The other three cations remain in solution and are free to react with exposed metallic surfaces.

The corrosion rate of lead/tin solders decreases with increase in tin content. Analysis of the electrolytes exposed to lead/tin solders shows that lead is the main alloying element attacked. The corrosion rate of low tin solders is increased by increasing the concentration of ethanediol in the range 15% to 50%, the corrosion rates of the low tin alloys in 50% ethanediol being similar to those in tap water only. This indicates that ethanediol in tap water, in the range 15% - 50%, acts as a mild corrosion inhibitor.

Aluminium was found to suffer localized corrosion when exposed along with lead/tin alloys to a chloride containing solution of either double distilled water or 50% ethanediol. From an investigation using a Jeol

35C electron microscope microprobe, lead was found to deposit on the aluminium surface after an induction period of 60 - 70 seconds, pits appearing almost simultaneously with the lead deposit.

Experimental work using the double corrosion cell equipment where aluminium foil was exposed to various lead halide containing solutions, confirmed that lead deposition did not occur until after an induction period of 60 - 70 seconds, but the aluminium corrosion potential (Ecorr) in each case was seen to shift in the noble direction immediately the lead halide solution was added to the aluminium cell. The degree of shift of the aluminium corrosion potential in the noble direction seems to be proportional to the lead concentration for lead fluoride, bromide and iodide solutions. In the case of lead chloride test solutions, at lead chloride concentrations of 20 ppm and above, the corrosion potential rose rapidly above the pitting corrosion potential (Ep) and then fell back to the Ep value and oscillated around this value. The results of the copper II chloride solutions were similar to those for lead chloride, except that the corrosion potential exceeded the Ep value at a copper chloride concentration of 2 ppm, a far lower concentration than that for lead. This would be expected from its position in the electrochemical series compared with that of lead.

As great care was taken to ensure that the halide concentration of the internal and external cell solutions for the lead halide and copper chloride tests were identical, and the activities of the two solutions were found to be the same, the shift in corrosion potential must be due to the presence of the heavy metal cations in solution. It is proposed that this corrosion potential shift is due to the movement

of heavy metal cations into the outer Helmholtz plane of the aluminium double layer causing a change in the distribution of the Al^{3+} cations since they will have different ionic radii, charge number and, more importantly, greater electron affinity compared with aluminium cations. This change of charge distribution will cause a redistribution of the electrons in the inner Helmholtz plane and hence a change in the corrosion potential.

The nobility of the critical pitting potential of aluminium in solutions of the halides increases in the order Cl < Br < I and F. From the anion sizes of the halides the sequence was expected to be F < Cl < Br < I. It will be noted that fluoride is the only one out of sequence.

It is suggested that a protective film of aluminium oxy-fluoride or aluminium hydroxy fluoride, forms on aluminium exposed to fluoride containing solutions, and that this film causes the shift in the critical potential to a more noble value.

An increase in solution temperature in the range 25°C to 75°C causes a decrease in nobility of the critical pitting potential of aluminium in fluoride, chloride and bromide solutions. The largest decrease in critical pitting potential with temperature rise occurs for aluminium samples exposed to fluoride containing solutions, indicating that the passive aluminium oxy-hydroxy fluoride film formed at 25°C is breaking down.

Increasing the concentration of the four halides in the range 0 - 125 ppm

caused a decrease in the nobility of the pitting corrosion potential of aluminium placed in either double distilled water or 50% ethanediol. The nobility of the Ep of aluminium in 50% ethanediol compared with double distilled water halide containing solution was slightly lower.

Basically all metals will corrode if their corrosion potential (Ecorr) in the test solution or working environment becomes more noble than their critical pitting potential (Ep) for that solution or working environment.

The present work demonstrates that with the exception of fluoride, all the other halide anions under consideration, bromide, chloride and iodide, not only determined the Ep of aluminium by their solution concentration and degree of aggression (anion size), but also have an effect on the corrosion potential, Pryor [62], Haynie and Ketcham[63]. The corrosion potential becomes more active with increasing halide aggression e.g. chloride being more aggressive than bromide. Hence, if halide anions are present in a sufficient concentration, which is dependent on their degree of aggression, they would initiate localized corrosion of aluminium. The concentration of halide ions required to initiate localized corrosion would be much higher than those levels commonly found in the drinking water (> 25 ppm) which is used to make up the 50% ethanediol coolant. These conclusions are in agreement with work done on chloride solutions by Ergang and Masing [58, 59], Maesche [60], Uhlig [36, 17] and Cocks [65].

A secondary source of halide anion contamination would, therefore, be required to initiate localized attack. This in the case of the auto-

mobile cooling system could come from halide containing flux residues left in the system from the lead/tin alloy soldering operation. Even if the level of halide contamination from flux residues is not sufficient to initiate localized corrosion of aluminium by corrosion potential and critical pitting potential shift, it will decrease the gap between the Ecorr value and the Ep value thus increasing the susceptibility of the aluminium to localized corrosion. An effective washing system for all components which undergo a soldering operation before attachment to a cooling system containing aluminium heat exchangers is therefore essential.

It has been established that cations of lead and copper in halide containing solutions cause a movement of the corrosion potential of aluminium in the noble direction, the degree of movement increasing with increase in metal cation concentration, until the corrosion potential reaches the critical pitting potential for aluminium initiating pitting corrosion. Above this critical concentration of metal cations, the corrosion potential levels off and oscillates around the critical pitting potential. The critical concentration of metal cations required to move the natural corrosion potential to the critical pitting potential also depends on the position of the metal cations in the electrochemical series, the concentration required decreasing with nobility.

Therefore, aluminium, or any other potentially active metal, which forms a part of a heat exchanger system, would initially register a corrosion potential in the passive region when exposed to fresh coolant in a new cooling system. However, as the coolant flows over and around other metals in the system, the cation concentration of the

coolant gradually increases due to soluble corrosion reaction products. If the cations are of metals which have a greater nobility than aluminium, they will cause the corrosion potential of the aluminium to move in the noble direction, until the Ep value is achieved, initiating pitting corrosion. The concentration of cations required to initiate corrosion will be dependent on the halides present in the coolant and their concentrations.

The pitting corrosion potential also decreases in nobility with increase in test solution temperature. Therefore the critical concentration of metal cations required to initiate pitting will also decrease with increase in temperature of the cooling system.

When a metal is being considered for use in contact with coolants, either water or 50% ethanediol, it is not only the pitting potential of the metal which must be considered, but also all the possible soluble contaminants, i.e. corrosion reaction products and flux residues, which will cause the corrosion potential to shift in the noble direction, disrupting an otherwise stable system. Careful selection of the composition of the noble metals and alloys in contact with the coolant will allow far more flexibility in the use of potentially active metals in the system, even if the corrosion inhibitor levels in the cooling system drop below a safe level for a short period of time. Aluminium has been found to have good corrosion resistance to attack by 50% ethanediol, only suffering localized attack if lead cations are present, and would probably perform very well in an uninhibited 50% ethanediol cooling system which had a halide level below 100 ppm. The degree of lead cation contamination of the coolant could be maintained below

the critical concentration of approximately 20 ppm, necessary for the initiation of localized attack of aluminium, by using high tin content solder in the joints which have a much lower corrosion rate than the low tin content solders normally used. Decreasing the coolant temperature would also have a beneficial effect by increasing the nobility of the aluminium pitting potential and hence increasing the critical concentration of lead required to initiate attack.

Fluoride has been found to attack aluminium generally not locally, in agreement with the observation by Lorking[71]. The corrosion reaction products are insoluble at lower temperatures (25°C - 50°C), forming a white tenacious coating on the aluminium effectively suppressing corrosion and shifting the pitting potential to more noble values. At lower temperatures, these stable complex films, dependent on their thickness, could be used as a form of limited protection for the aluminium against other aggressive anions.

These films could be used to protect aluminium products exposed to coolants or electrolytes containing aggressive anions at temperatures below 50°C. The heat exchangers or components could be filled with a fluoride containing solution and polarized to a potential which stimulates thick film formation on the internal areas of the component. After film formation, the component could be flushed out with water to remove excess soluble fluoride and then connected to the cooling system. At temperatures in excess of 50°C, there is a dramatic shift in the critical pitting potential of aluminium in fluoride containing solution to less noble potentials, indicating complex film breakdown. Therefore, complex films formed under standard conditions in sodium

fluoride containing solution could not be used to protect aluminium against aggressive anions at temperatures in excess of 50°C.

6.1 SUGGESTIONS FOR FURTHER WORK

(a) A protective fluoride oxy-hydroxy film forms on aluminium at various potentials in sodium fluoride solutions. This film is of limited stability; breaking down at temperatures in excess of 50°C in ethanediol solutions. Investigations into methods of improving the stability of this film, possibly by the incorporation of other metals into the film which form in soluble fluoride salts, would be of interest.

(b) When aluminium is exposed to lead halide solutions an induction period has been found during which the corrosion potential shifts to more noble values, it would be of interest to determine the part played by halide anions during this period using radioactive tracer techniques.

(c) The film which forms in the 100 ppm sodium fluoride double distilled water solution is different in thickness and apparent structure from that formed in 100 ppm sodium fluoride 50% ethanediol solution at the same potential. Auger and E.S.C.A.N. analysis of the surface film could be carried out to determine the difference between the two films.

(d) Ethanediol has been found to act as a mild corrosion inhibitor in the range 15% to 50%. Infra red spectrophotometry analysis could be used to determine whether organo-metallic compounds form on the surface.

(e) Evaluate the critical concentration of lead and copper required to initiate localized corrosion of aluminium in bromide, fluoride and iodide containing solutions. The critical concentration of lead and copper in chloride containing solutions has been determined, this could be repeated for bromide, fluoride and iodide containing solutions.

REFERENCES

1 G. Okamoto, K. Tachibana, S. Nishiyama, T. Sugita, Passivity And Its Breakdown Of Iron and Iron Base Alloys - NACE, Houston, Texas (1976) p. 106

2 H. Strehblow, B. Titze, B.P. Lochel, Corrosion Science 19 (1979) p. 1047

3 U. Bertocci, J.L. Mullen, Y.X. Ye 5th Intern. Symposium On Passivity, Bombonnes, France, June 1983

4 U.R. Evans, J. Chem. Soc. (London) p. 1020 (1927)

5 S.C. Britton and U.R. Evans, J. Chem. Soc. (London) p. 1773 (1930)

6 R.L. Burwell and T.P. May, Trans. Electrochem. Soc. 94 p. 195 (1948)

7 I.L. Rosenfeld and I.S. Danilov, Corrosion Sci. 7 p. 129 (1967)

8 T.P. Hoar, D.C. Mears and G.P. Rothwell, Corrosion Sci. 5, p.279 (1965)

9 J. Augustynski, J. Electrochem. Soc., U.S.A. (1978) p. 989

10 S. Meitra, E.D. Verink, J. Electrochem. Soc., U.S.A. (1978) p. 309

11 T.E. Pou, O.J. Murphy, J.O.M. Bockris, L.L. Tangson, M. Monkowski, in press.

12 G.C. Wood, J.A. Richardson, M.F. Abd. Rabbo, L.B. Mapa, W.H. Sutton, J. Electrochem. Soc., U.S.A., (1978), p. 973.

13 S. Szklarska Smialowska, H. Viefhaus, M. Janik-Czachor, Corrosion Sci. 16 (1976), p. 644

14 M. Janik - Czachor, K. Kaszczyszyn, Werkstoffe und Korrosion 33 (1982), p. 500

15 B.P. Lochel, H.H. Strehblow, Electrochimica Acta 28 (1983) p. 565

16 B.P. Lochel, H.H. Strehblow, Fall Meeting Of The Electrochem. Soc., Washington D.C., October 1983

17 H. Bohni and H.H. Uhlig, J. Electrochem. Soc. 116 p. 906 (1969)

18 J.M. Kolotyrkin, J. Electrochem. Soc. 108, p. 209 (1961)

19 T.P. Hoar and W.R. Jacob Nature 216, p. 1299 (1967)

20 W. Khalil, H.H. Strehblow - to be published.

21 Curme, G.O. and Young, C.O. Ind. Eng. Chem. 1925, 17, p. 1117 - 1120

22 N. Sato, Electrochimica Acta 16, p. 1683 (1971)

23 T.P. Hoar, Corrosion Sci. 7, p. 341 (1967)

24 C.Y. Chao, L.F. Lin, D.D. MacDonald, J. Electrochem. Soc. 128 (1981), p. 1187

25 J.A. Richardson and G.C. Wood, Corrosion Sci. 10, p. 313 (1970)

26 E.C. Pearson, H.J. Huff and R.H. Hay, Can, J. Technology 30, p. 311 (1952)

27 L. Gainer and G. Wallwork, A Review Of Pitting Corrosion Theories

28 M. Pourbaix, "Localized Corrosion", p. 12 Nace - 3 Houston (1974)

29 T. Suzuki, M. Yanabe and Y. Kitamura, Corrosion 29, p. 18 (1973)

30 S. Szklarska - Smialowska, Brit. Corr. J. 10, p. 11 (1975)

31 R.P. Frankenthal and H.W. Pickering, J. Electrochem. Soc. 119, p. 1304 (1972)

32 M.J. Pryor "Localized Corrosion", p. 2 Nace 3 - Houston (1974)

33 B. Verkerk, Unesco Int. Conf. on Radioisotopes In Scientific Research, UNESCO/BS/RIC44

34 H.H. Strehblow "7th International Congress On Metallic Corrosion" 1984, Vol. 2, p. 99

35 W.E. Cooke and H. Bowman "11th International A.W.S. - W.R.C. Brazing Conference", Los Angeles, C.A., 14-16th April, 1980

36 H.P. Leckie and H.H. Uhlig, J. Electrochem. Soc. 113, p. 1262 (1966)

37 J.M. Kolotyrkin, Corrosion 12, p. 261 (1963)

38 L.F. Lin, C.Y. Chao, D.D. MacDonald, J. Electrochem. Soc. 128, (1981), p. 1194

39 J.A. Richardson and G.C. Wood, J. Electrochem. Soc. 120, p. 193 (1973)

40 G.C. Wood, W.H. Sutton, J.A. Richardson, T.N. Riley and A.G. Malherbe, "Localized Corrosion", p. 526, NACE - 3 Houston (1974)

41 J. Zahavi and M. Metzger, J. Electrochem. Soc. 121, p. 268 (1974)

42 T.P. Hoar, Discussions Faraday Soc. 1, p. 299 (1947)

43 I.L. Rosenfeld, Korrozja I Zashch, Metallov, Moscow (1970)

44 M. Pourbaix, L. Klimzack-Mathieu, Ch. Martens, J. Meunier, Ch. Vanlengenhaghe, L. de Munch, J. Laureys, L. Nellmans and M. Warzee, Corros. Sci. 3, p. 217 (1963)

45 N.D. Tomashov, G.P. Chernoua and O.N. Markova, Corrosion 20, p. 166 (1964)

46 M. Prazak, J. Tousek and W. Spanily, Zashch Metallov 5, p. 371 (1969)

47 A. Desestret, Corros. Trait, Prot, Fin., 15, p. 281 (1967)

48 P. Leckie, J. Electrochem. Soc., 117, p. 1152 (1970)

49 B.E. Wilde and E. Williams, Electrochim, Acta, Vol. 16, p. 1971 (1971)

50 J.M. Kolotyrkin and L.I. Freiman, Dokl, Akad, Naud, S.S.S.R. 162, p. 376 (1965)

51 Smialowska and Czachor "Localized Corrosion" NACE 3 - Houston, p. 353 (1974)

52 W. Schwenk, Corrosion 20, 129 (1964), and Corrosion Sci. 5, p. 245 (1965)

53 G. Herbsleb, Werkstoffe und Korrosion, 16, p. 929 (1965)

54 P. Forchhammer and H.J. Engell, Werkstoffe und Korrosion 21, 1, (1969)

55 Z. Szklarska - Smialowska, Bull. Acad. Pol. Sci., XIII, 221 (1965)

56 Z. Szklarska - Smialowska and M. Janik-Czachor, Corrosion Sci. 7, p. 65 (1967)

57 W.H. Sutton, PhD Thesis, Manchester University 1970

58 R. Ergang and G. Masing, Z. Elektrochem., 53, p. 160 (1951)

59 D. Altenpohl and G. Masing, Z. Metallkunde, 43, p. 433 (1952)

60 H. Kaesche, Z. Physik, Chem., N.F., 34, p. 87 (1962)

61 E.M. Khairy and M.K. Hussinn, Corrosion, 13, p. 793 (1957)

62 M.J. Pryor, J. Electrochem. Soc., 62, p. 782 (1958)

63 F.H. Haynie and S.J. Ketcham, Corrosion, 19, p. 403 (1963)

64 D.E. Davies, J. Appl., Chem., 9, p. 656 (1959)

65 F.H. Cocks (Giner, Inc., Waltham, M.A. [U.S.A.]) July 1981

66 Stella M. De Micheli, Corrosion Sci., Vol. 18, p. 605 (1978)

67 S. Dallek and R.T. Foley, J. Electrochem. Soc., Vol. 123, No. 12, p. 1776 (1976)

68 F.D. Bogar and R.T. Foley, J. Electrochem. Soc. 119, p. 462 (1972)

69 Z.A. Foroulis and M.J. Thubrikar, J. Electrochem. Soc. 122, p. 1296 (1965)

70 K.J. Laidler, "Chemical Kinetics" 2nd Ed., p. 286 McGraw-Hill, New Yrok (1965)

71 K.F. Lorking and J.E.O. Mayne, Brit. Corr. J. 1, p. 181 (1966)